
Masters Theses

Student Theses and Dissertations

1969

Tunnel diode models for electronic circuit analysis program (ECAP)

Carmon Dale Thiems

Follow this and additional works at: https://scholarsmine.mst.edu/masters_theses



Part of the [Electrical and Computer Engineering Commons](#)

Department:

Recommended Citation

Thiems, Carmon Dale, "Tunnel diode models for electronic circuit analysis program (ECAP)" (1969). *Masters Theses*. 7002.
https://scholarsmine.mst.edu/masters_theses/7002

This thesis is brought to you by Scholars' Mine, a service of the Missouri S&T Library and Learning Resources. This work is protected by U. S. Copyright Law. Unauthorized use including reproduction for redistribution requires the permission of the copyright holder. For more information, please contact scholarsmine@mst.edu.

TUNNEL DIODE MODELS FOR
ELECTRONIC CIRCUIT ANALYSIS PROGRAM (ECAP)

BY 541

CARMON DALE THIEMS , 1938-

A

THESIS

submitted to the faculty of

THE UNIVERSITY OF MISSOURI - ROLLA

in partial fulfillment of the requirements for the

Degree of

MASTER OF SCIENCE IN ELECTRICAL ENGINEERING

Rolla, Missouri

1969

T. 2274

~~68~~

68 pages

Approved by

Frank J. Kern (Advisor) E C Bertnoll
Loumy B. Whirich

TABLE OF CONTENTS

	Page
LIST OF FIGURES.....	iii
LIST OF PHOTOGRAPHS.....	v
LIST OF TABLES.....	vi
 I. INTRODUCTION.....	 1
 II. MODELS AND CURRENT-VOLTAGE CHARACTERISTICS.....	 4
 III. MODELS IN CIRCUIT APPLICATIONS.....	 17
 IV. CONCLUSIONS.....	 30
 APPENDIX I-SUMMARY OF MODELING OF ACTIVE DEVICES FOR COMPUTER-AIDED CIRCUIT DESIGN.....	 34
 REFERENCES.....	 43
 APPENDIX II-ANALYSIS, CALCULATION AND SELECTION OF PARAMETERS FOR TUNNEL DIODE MODELS.....	 45
 BIBLIOGRAPHY.....	 59
 VITA.....	 62

LIST OF FIGURES

		Page
Figure 1	Tunnel Diode Current-Voltage Characteristics	1
Figure 2	Model 1 Current-Voltage Characteristics	4
Figure 3	Model 1	6
Figure 4	Model 1 Current-Voltage Curve	7
Figure 5	Model 2 Current-Voltage Characteristic	8
Figure 6	Model 2	9
Figure 7	Model 2 Current-Voltage Curve	11
Figure 8	Model 3 Current-Voltage Characteristic	12
Figure 9	Model 3	13
Figure 10	Model 3 Current-Voltage Curve	16
Figure 11	Relaxation Oscillator	17
Figure 12	Astable Multivibrator	19
Figure 13	Model 1 Oscillator Output Waveform	21
Figure 14	Model 2 Oscillator Output Waveform	23
Figure 15	Model 3 Oscillator Output Waveform	25
Figure 16	Model 1 Multivibrator Output Waveform	27
Figure 17	Model 2 Multivibrator Output Waveform	28
Figure I-1	Diode Current-Voltage Characteristic	36
Figure I-2	Diode Models	37
Figure I-3	Ebers-Moll Model	38
Figure I-4	Beaufoy-Sparks Charge Control Model	39
Figure I-5	Linville Lumped Model	39
Figure I-6	Zener Diode Model	40

Figure I-7	Tunnel Diode Model	41
Figure II-1	Tunnel Diode Current-Voltage Characteristic	47
Figure II-2	Model 1	48
Figure II-3	Three Section Piecewise Linear Current Voltage Curve	49
Figure II-4	Model 2	52
Figure II-5	Five Section Piecewise Linear Current Voltage Curve	53
Figure II-6	Model 3	56
Figure II-7	Model 3 Current-Voltage Characteristic	57

LIST OF PHOTOGRAPHS

Photograph 1	TD-19 Current-Voltage Curve	Page 2
Photograph 2	TD-13 Current-Voltage Curve	2
Photograph 3	Oscillator Output Voltage Waveform	18
Photograph 4	Multivibrator Output Voltage Waveform	18

LIST OF TABLES

TABLE I	Model 1 ECAP Data	Page 5
TABLE II	Model 2 ECAP Data	10
TABLE III	Model 3 ECAP Data	15
TABLE IV	Model 1 Oscillator ECAP Data	20
TABLE V	Model 2 Oscillator ECAP Data	22
TABLE VI	Model 3 Oscillator ECAP Data	24
TABLE VII	Model 1 Multivibrator ECAP Data	26
TABLE VIII	Model 2 Multivibrator ECAP Data	26
TABLE II-1	Data From G.E. Data Sheet	46
TABLE II-2	Model 1 Parameter Values	50
TABLE II-3	Model 2 Parameter Values	55
TABLE II-4	Model 3 Parameter Values	58

I. INTRODUCTION

In this paper ECAP models for the tunnel diode are presented. Results showing the model, the current-voltage characteristics are discussed. Operation in typical circuits is presented. A summary of the current state of the art in modeling appears in Appendix I.

Since ECAP is only structured to accept piecewise-linear models of these devices, that type of model is presented here. All of the models are developed to approximate the typical tunnel diode current-voltage characteristic shown in Figure 1 and also in Photographs 1 and 2. In Figure 1, peak current (I_p) and peak voltage (V_p) identifies the point on the curve where the negative portion of the V-I curve begins and valley current and valley voltage identifies the point where the negative portion of the V-I curve ends. These models use controlled current sources to

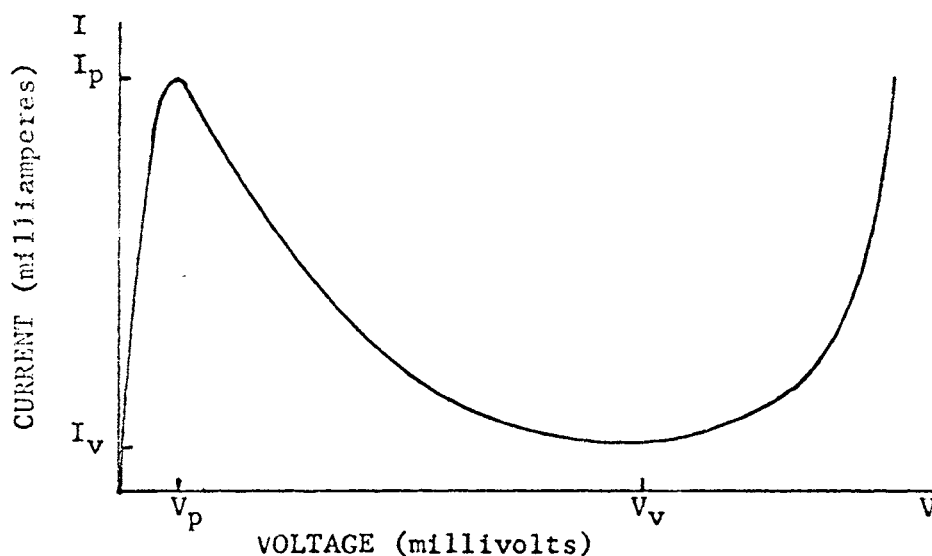
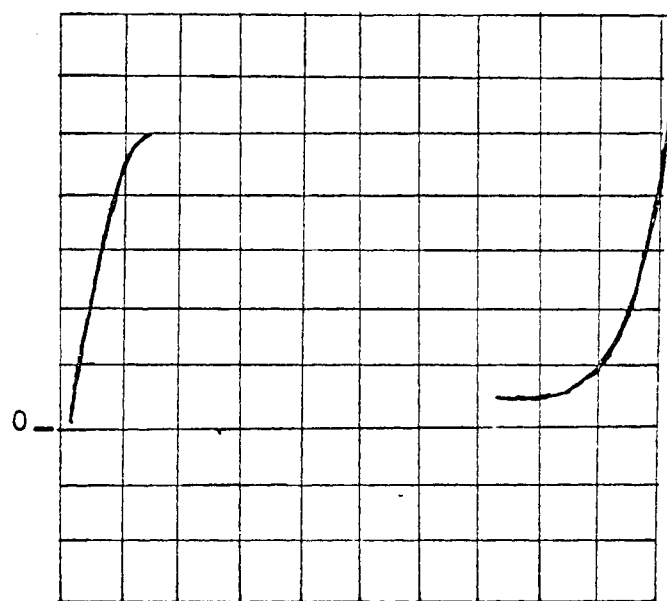
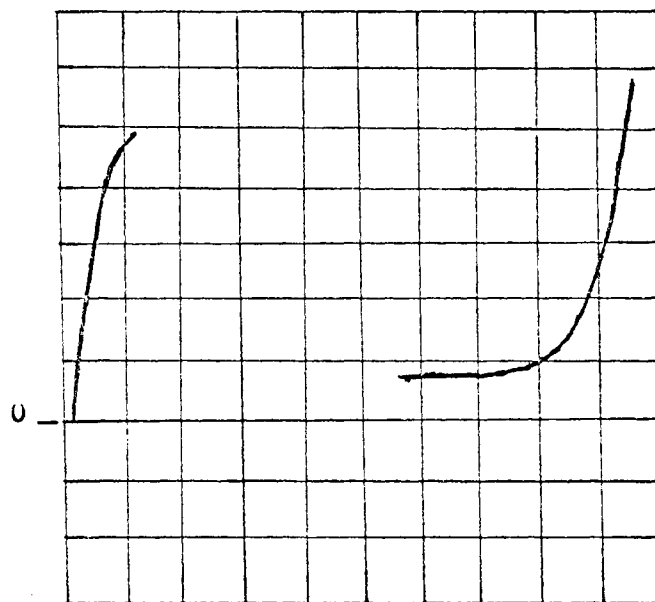


Figure 1 Tunnel Diode Current-Voltage Characteristics



Photograph 1 (traced) TD-19 Current Voltage Curve

CURRENT-2ma/cm
VOLTAGE-0.05v/cm



Photograph 2 (traced) TD-13 Current Voltage Curve

CURRENT-0.2ma/cm
VOLTAGE-0.05v/cm

realize the negative slope portion of these curves rather than the negative resistors used by other tunnel diode models.

The models shown in Figure 3, 6 and 9 use all of the available ECAP stored elements; resistors, inductors, capacitors, voltage sources, dependent current sources, and independent current sources. The method used to select the element values for a particular tunnel diode is discussed in Appendix II.

II. MODELS AND CURRENT-VOLTAGE CHARACTERISTICS

The first model shown in Figure 3 and its current-voltage curve in Figure 2 represent the simplest meaningful straight line approximation of the current voltage curve of the actual

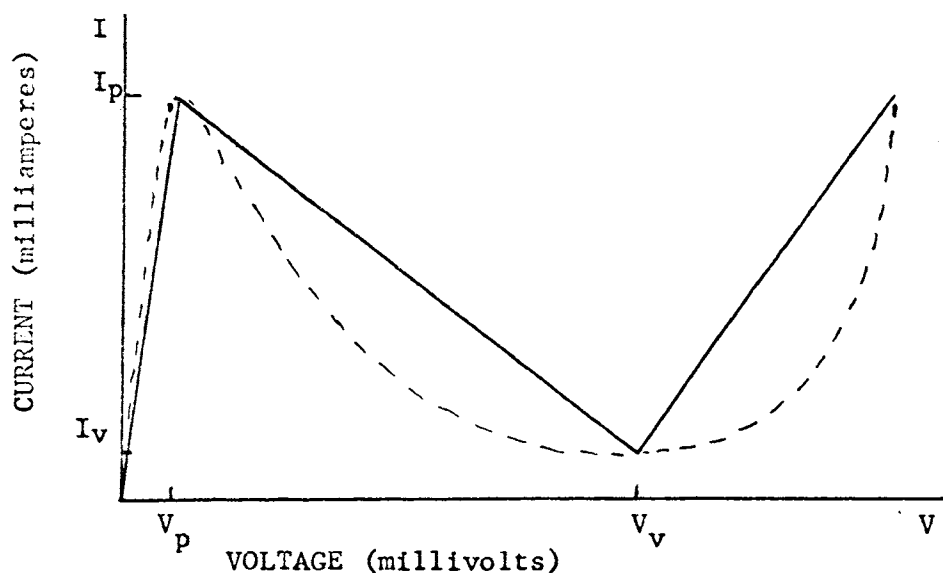


Figure 2 Model 1 Current-Voltage Characteristics

device.

The conductance G_1 shown in Figure 3 is the element which accounts for the positive slope line from $(0,0)$ to (V_p, I_p) . At that point the controlled current source with $-GM_1$ and controlled by current in R_3 is switched in the circuit S2 and provides the negative slope line from (V_p, I_p) to (V_v, I_v) . Then the controlled current source with GM_1 controlled by current in R_2 and current source $-I_1$ are switched in for the remaining positive slope line from (V_v, I_v) . The model is discussed in more detail in Appendix II.

The ECAP data in TABLE I describes the model of Figure 3 approximating TD-19 General Electric tunnel diode.

TABLE I Model 1 ECAP Data

```

      Transient Analysis
B1    N(1,2), R=(10E7,0.36)
B2    N(2,0), G=(0.154,0.058), E=(0,-0.355), I=(0,-0.00095)
B3    N(2,0), R=10E8
B4    N(2,3), R=10E8
B5    N(3,0), R=0.001, E=-0.065
B6    N(2,0), R=10E8, E=0.355
B7    N(2,0), C=27E-12
B8    N(4,1), L=0.8E-9
B9    N(2,3), R=10E8
C      *****
C      These three cards describe the voltage generator to
C      give the voltage sweep for determining the model V-A
C      characteristic.
B10   N(0,4), R=30, E=(1.5,0)
B11   N(4,0), C=0.05E-6
B12   N(4,0), R=10E8, E=(-0.45,0)
C      *****
T1    B(9,2), GM=(0,0.185)
T2    B(4,3), GM=(0,-0.185)
S1    E=1, (1), OFF
S2    E=5, (3,4), OFF
S3    E=6, (2,9), OFF
S4    E=12, (10,12), OFF

```

When determining the current-voltage characteristic of the model, B7 and B8 should be changed to the following:

```

B7    N(2,0), R=10E8
B8    N(4,1), R=0.001

```

This is required because the energy stored in the capacitor and inductor are of the same order of magnitude as the energy dissipated in the other elements and changing the direction of the voltage and current cause the capacitor and inductor to reverse bias the model. When used in a circuit these effects are normal and account for the internal inductance capacitance. The

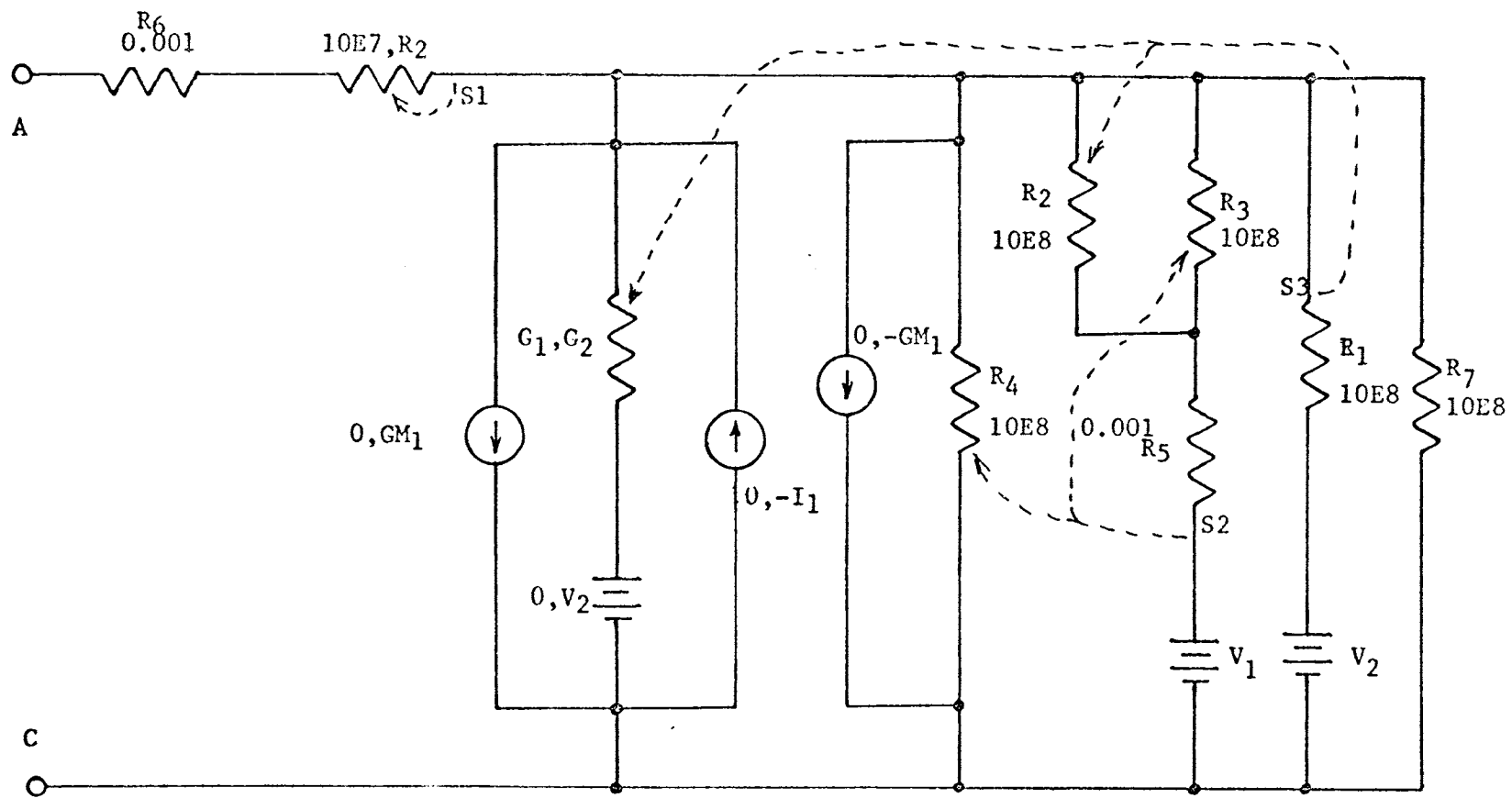


Figure 3 Model 1

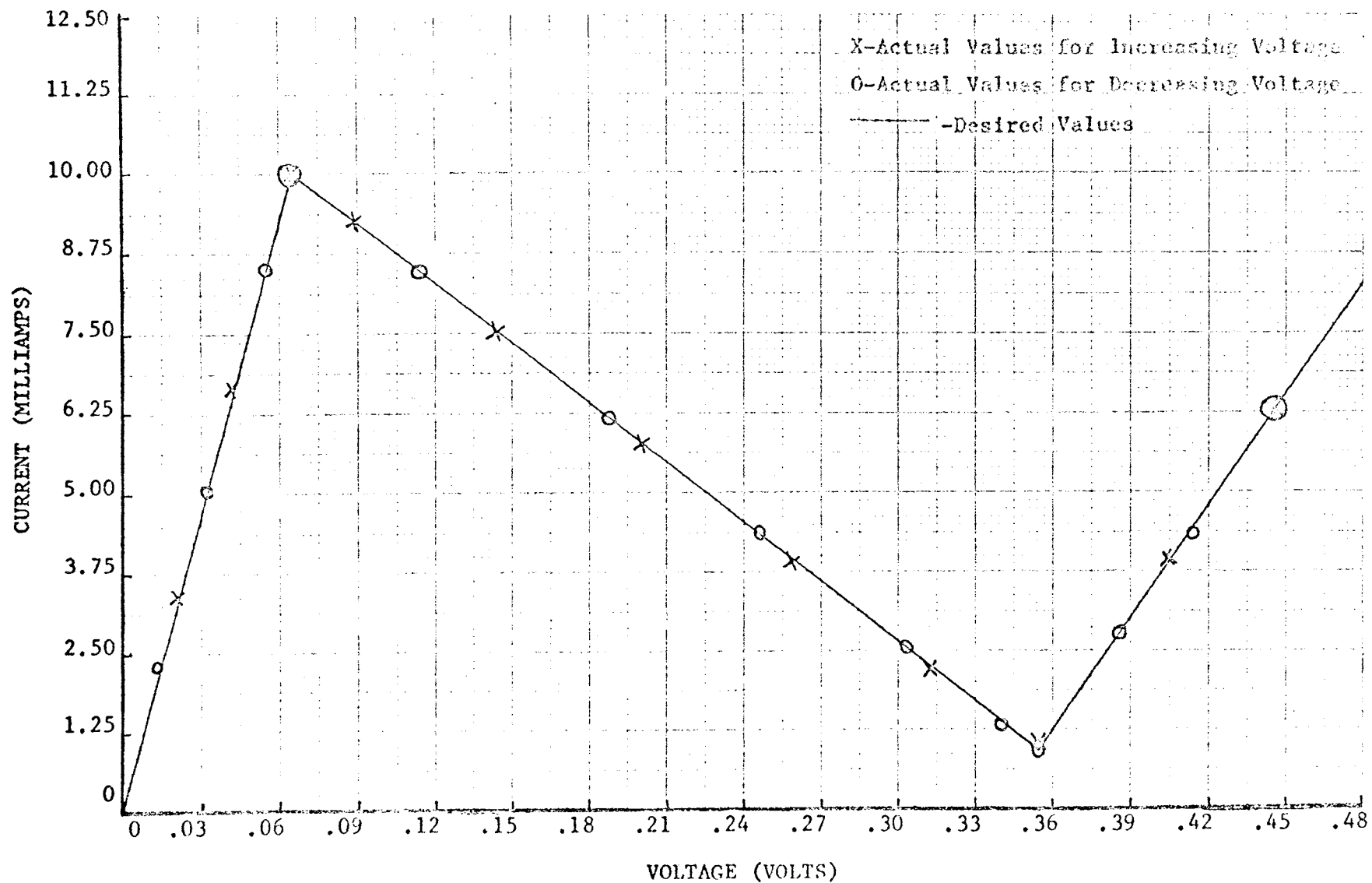


Figure 4 Model 1 Current-Voltage Curve

results of the ECAP program using this data are shown in Figure 4. The results verify that the desired curve has been generated. However when compared with the actual device current-voltage curve of Photograph 1, the model is seen to represent the actual device rather inaccurately as expected.

The second model shown in Figure 6 with the current-voltage curve in Figure 5 represents a modified straight line approximation of the current-voltage curve of the actual device which will give a more exact approximation of the actual device characteristic.

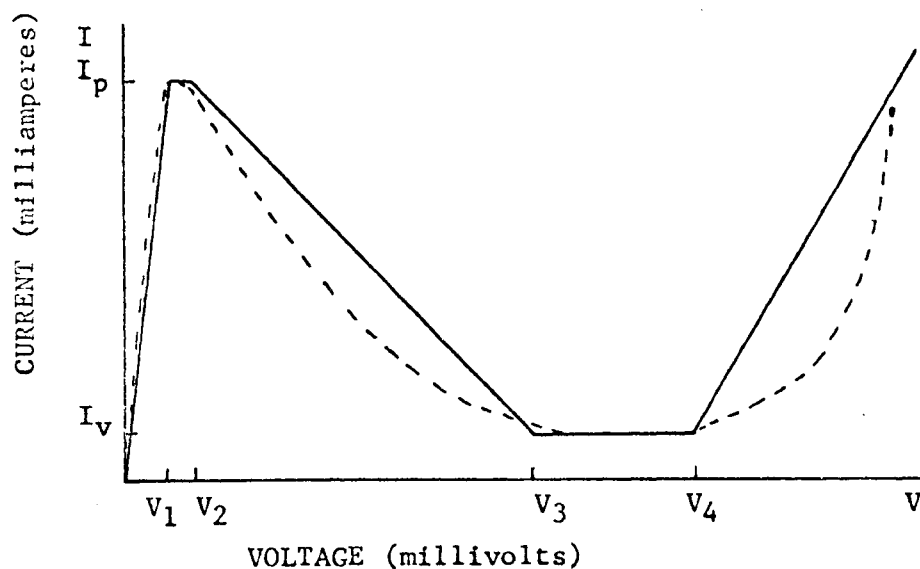


Figure 5 Model 2 Current-Voltage Characteristic

The conductance G_1 shown in Figure 6 provides the positive slope line from $(0,0)$, to (V_1, I_p) . Switch S_2 changes G_1 and switches in the current source $-I_1$ to provide the constant current line from (V_1, I_p) to (V_2, I_p) . Switch S_3 then turns on the con-

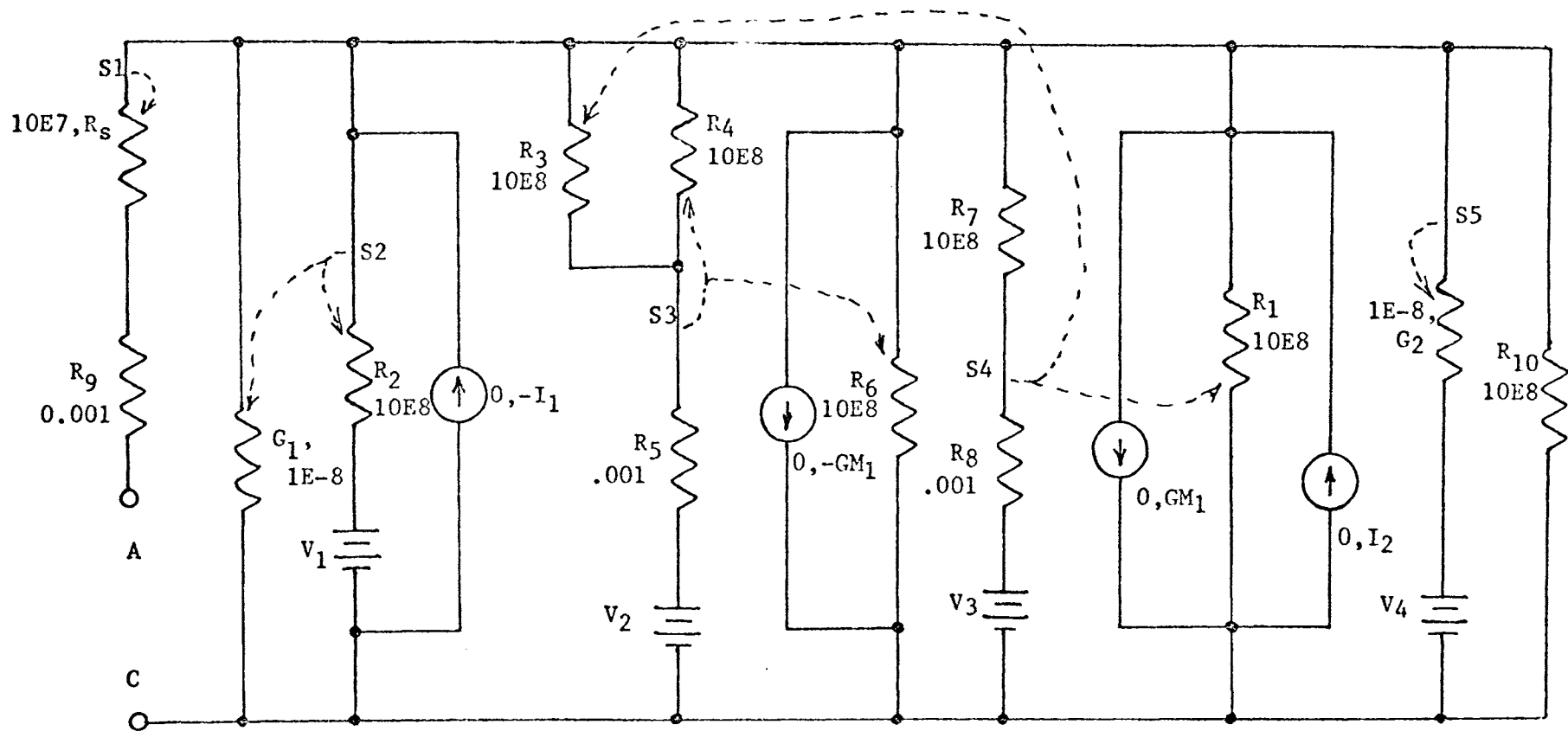


Figure 6 Model 2

trolled current source $-GM_1$ controlled by current in R_4 . This provides the negative slope line from (V_2, I_p) to (V_3, I_p) . The constant current line for (V_3, I_v) to (V_4, I_v) is generated with GM_1 controlled current source controlled by R_3 current, and current source I_2 being turned on by switch S_4 . The conductance G_2 turned on by switch S_5 generates the positive slope line from (V_4, I_v) .

The model is discussed in more detail in Appendix II.

The ECAP data in TABLE II describes the model of Figure 6.

TABLE II Model 2 ECAP Data

```

Transient Analysis
B1      N(1,2), R=(10E7,0.36)
B2      N(2,0), G=(0.161,1E-8)
B3      N(2,0), R=10E8, E=-0.0618, I=(0,-0.01)
B4      N(2,3), R=10E8
B5      N(3,0), R=0.001, E=-0.0682
B6      N(2,0), R=10E8
B7      N(2,4), R=10E8
B8      N(4,0), R=0.001, E=-0.249
B9      N(2,0), R=10E8, I=(0,0.00905)
B10     N(2,0), G=(1E-8,0.0887), E=-0.408
B11     N(2,0), C=27E-12
B12     N(5,1), L=0.8E-9
B13     N(2,3), R=10E8
C       *****
C       These three cards describe the voltage generator to
C       give the voltage sweep for determining the model V-A
C       characteristic.
B14     N(0,5), R=30, E=(1.5,0)
B15     N(5,0), C=0.05E-6
B16     N(5,0), R=10E8, E=(-0.45,0)
C       *****
T1      B(4,6), GM=(0,-0.0492)
T2      B(13,9), GM=(0,0.0492)
S1      B=1, (1), OFF
S2      B=3, (2,3), OFF
S3      B=5, (4,6), OFF
S4      B=8, (9,13), OFF
S5      B=10, (10), OFF
S6      B=16, (14,16), OFF

```

When determining the current-voltage characteristic of this

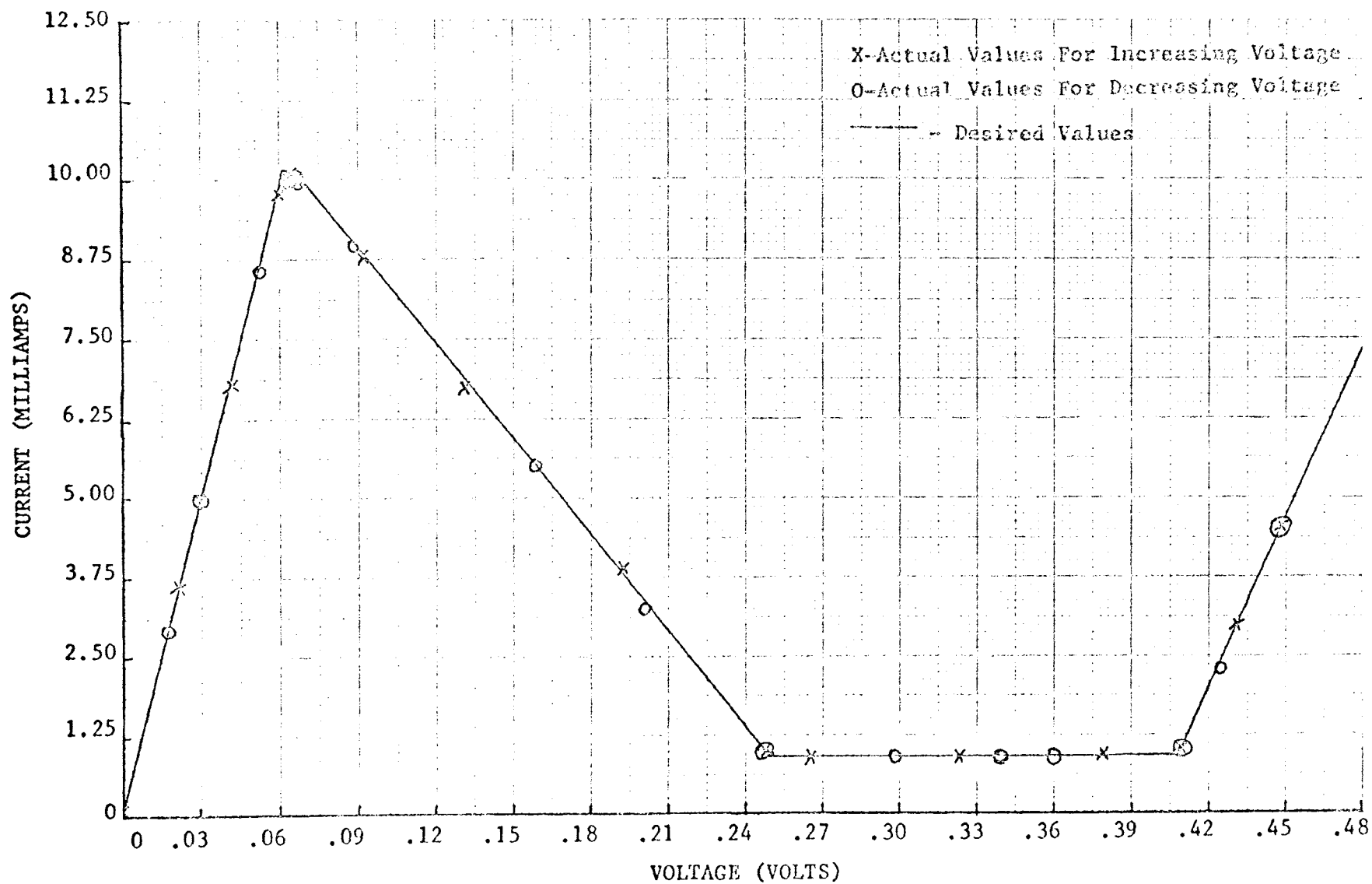


Figure 7 Model 2 Current-Voltage Curve

model as with the first model, the capacitor and inductor must be removed and replaced with an open and short respectively. B11 and B12 should be changed as follows:

B11 N(2,0), R=10E8
 B12 N(5,1), R=0.001

The results of the ECAP program using the second model are shown in Figure 7. The results verify that the desired curve has been generated. In comparison with Photograph 1, the current-voltage curve of the actual device, it is evident that this model does give a more exact approximation of the actual device characteristic.

A third model is shown in Figure 9 and its current-voltage curve in Figure 8 uses resistor-capacitor time constant effects to eliminate the straight lines and sharp corners of the other two models.

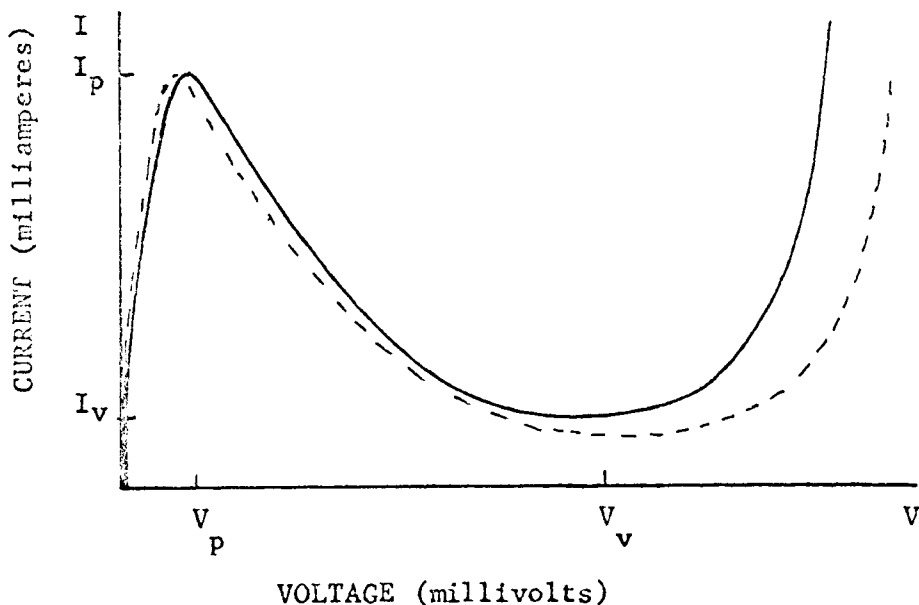


Figure 8 Model 3 Current-Voltage Characteristic

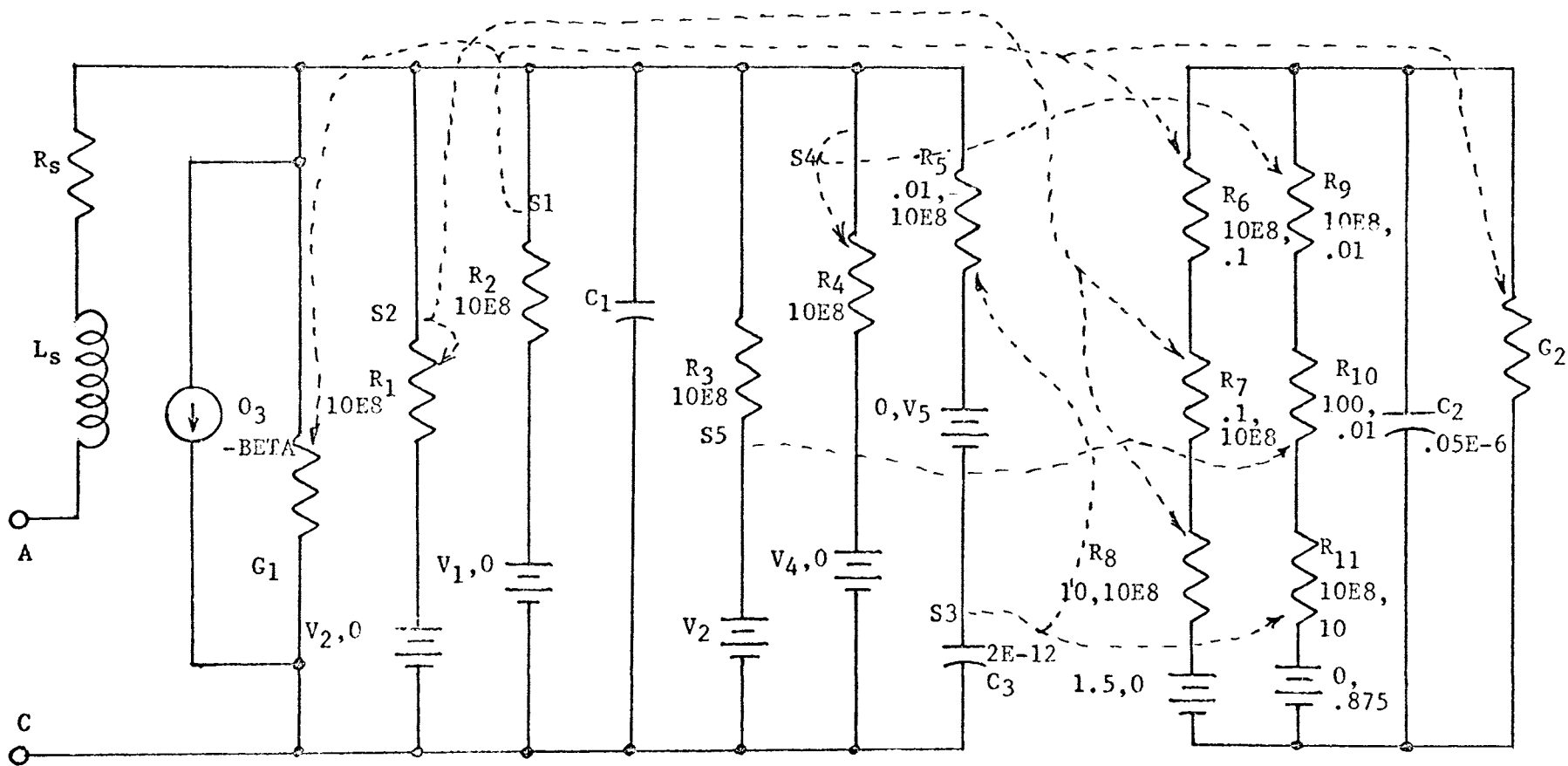


Figure 9 Model 3

The conductance G_1 provides the curve from $(0,0)$ to (V_p, I_p) . The negative slope portion of the characteristic from (V_p, I_p) to (V_v, I_v) is generated when S1 turns on the -BETA controlled current source, controlled by current in G_2 , switch S2 turns off R_3 to provide the remainder of the curve from (V_v, I_v) . This completes the characteristic for increasing voltage. However this model unlike Models 1 and 2, uses a different portion of the circuit for decreasing voltage. S4 and S5 turned on during increasing voltage but are used for the decreasing portion of the curve. When the voltage reaches the maximum and starts to decrease switch S3 turns off. C_2 is allowed to charge up again increasing current in G_2 , decreasing it in controlled current source. When switch S5 turns off as the voltage decreases the C_2 capacitor stops charging up discharge reducing current in G_2 and increasing current in G_1 . This action is what gives the characteristic its premature rise of current. This will be discussed in greater detail in Appendix II.

The ECAP coding of TABLE III describes the model of Figure 9.

The results of ECAP program using the third model are shown in Figure 10. This model for increasing voltage duplicates the actual device closely, however, there is a large discrepancy on retracing the curve for falling voltage.

The first two models shown use the same components to approximate the tunnel diode during the rising and falling of voltages. The third model, however, uses part of its elements during rising voltages and part during falling voltage. In selecting one of these models, the desired accuracy is the basic criterion.

TABLE III Model 3 ECAP Data

```

      Transient Analysis
E1      N(1,2), L=0.8E-9
E2      N(2,3), R=0.36
E3      N(3,0), G=0.154
E4      N(3,0), R=10E8, E=(-0.355,0)
E5      N(3,0), R=10E8, E=(-0.065,0)
E6      N(3,0), C=27E-12
E7      N(3,0), R=10E8, E=-0.355
E8      N(3,0), R=10E8, E=(-0.408,0)
E9      N(3,8), R=(0.01,10E8), E=(0,-0.45)
B10     N(8,0), C=2E-12
B11     N(0,4), R=(10,10E8), E=(1.5,0)
B12     N(4,5), R=(10E8,0.1)
B13     N(5,6), R=(0.1,10E8)
B14     N(7,6), R=(100,0.01)
B15     N(9,7), R=(10E8,0.01)
E16     N(0,9), R=(10E8,10), E=(0,0.875)
E17     N(6,0), C=0.05E-6
E18     N(6,0), G=0.308
C      *****
C      These three cards describe the voltage generator to
C      give the voltage sweep for determining the model V-A
C      characteristic.
E19     N(0,1), R=(10,10E8), E=(1.5,0)
B20     N(1,0), C=0.05E-6
E21     N(1,0), R=10E8, E=(-0.45,0)
C      *****
T1      B(18,3), BETA=(0,-0.8)
S1      B=5, (3,5,12,18), OFF
S2      B=4, (4,11,13), OFF
S3      B=10, (9,16), ON
S4      B=8, (8,15), OFF
S5      B=7, (14), OFF
S6      B=21, (19,21), OFF

```

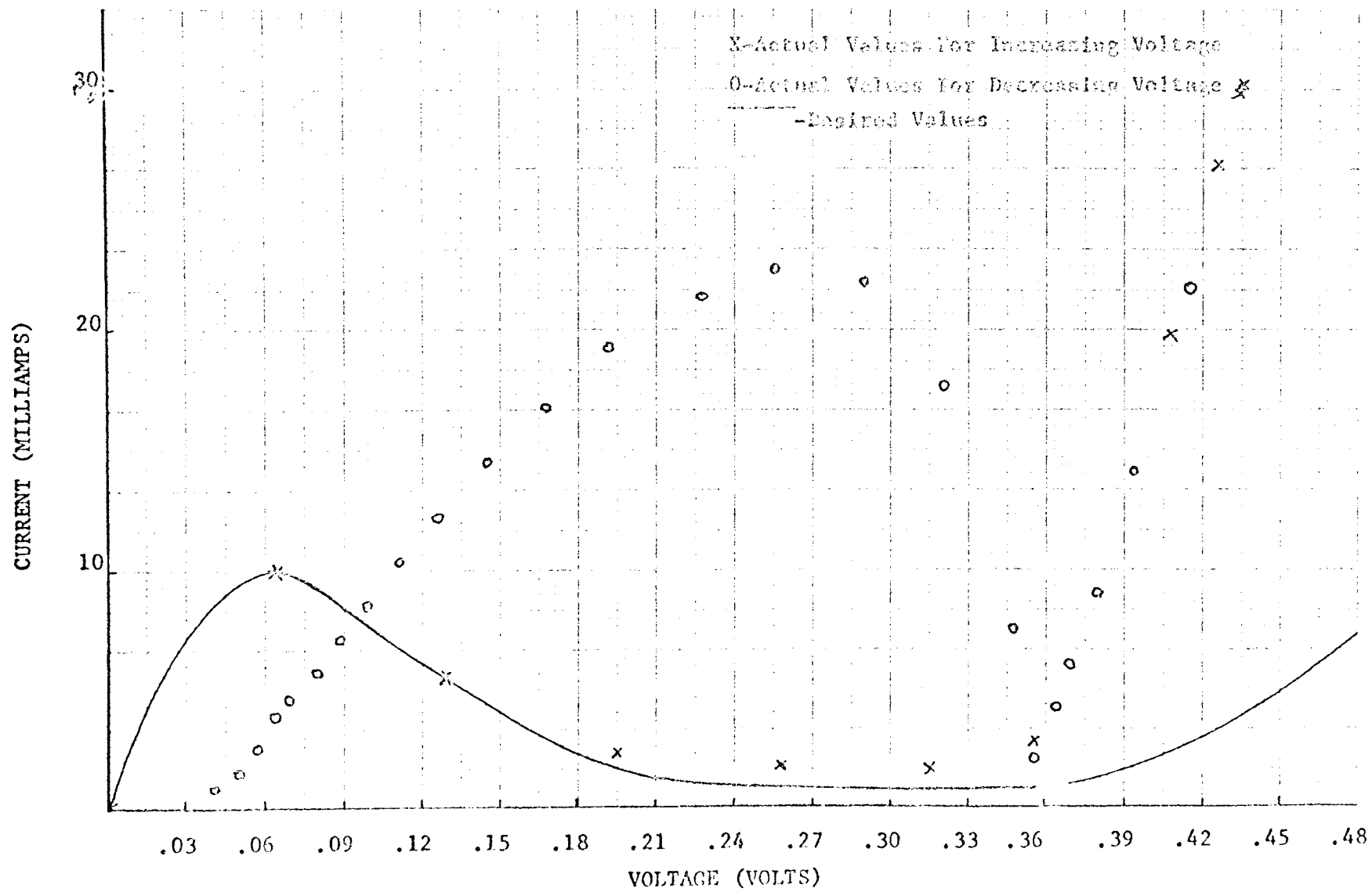


Figure 10 Model 3 Current-Voltage Curve

III. MODELS IN CIRCUIT APPLICATIONS

All three models were tested in various tunnel diode circuits. A relaxation oscillator circuit Figure 11 and astable multivibrator circuit Figure 12 were used.

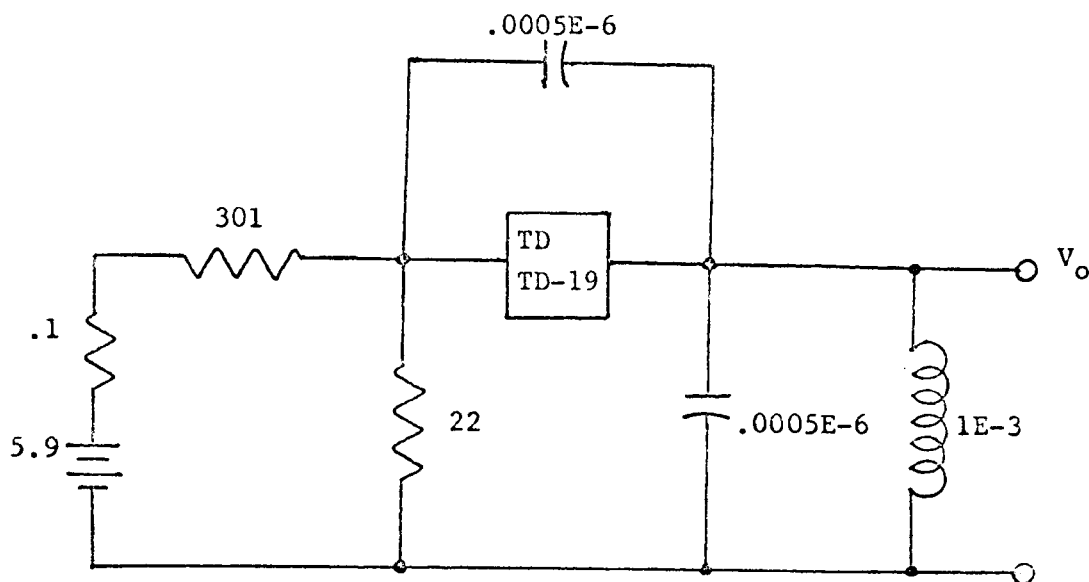
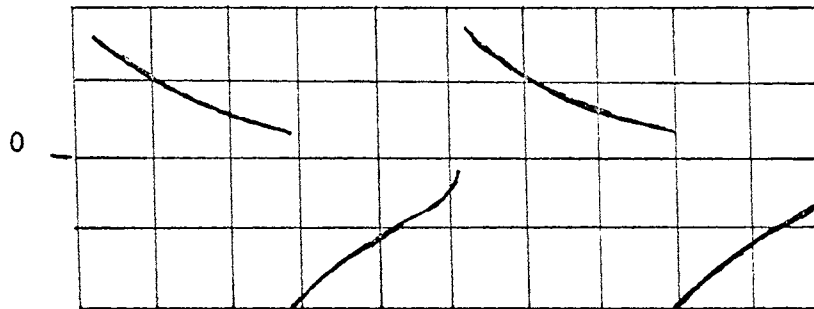


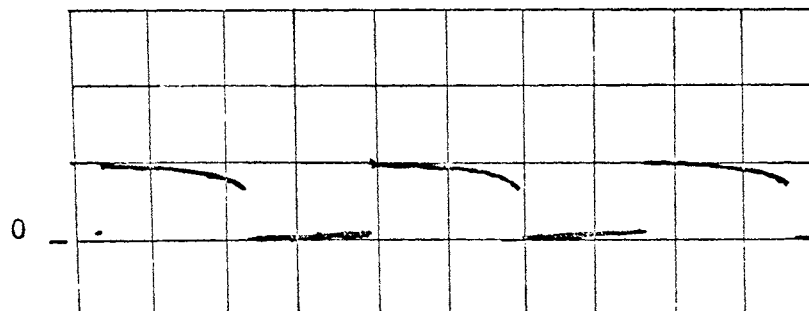
Figure 11 Relaxation Oscillator

In the operation of the relaxation oscillator the output voltage initially jumps to a level of approximately .4 volts. The voltage decays during which time the tunnel diode voltage is increasing. When the tunnel diode voltage reaches peak volt the output voltage goes negative due to the effect of the capacitor inductor circuit. At the same time the tunnel diode voltage has increased to greater than valley voltage (V_v). The output voltage decays and when the tunnel diode voltage decays to valley voltage the output voltage jumps positive and repeats. This circuit output voltage is shown in Photograph 3.



Photograph 3 (traced) Oscillator Output Voltage Waveform

VOLTAGE-0.2v/cm
TIME-20u sec/cm



Photograph 4 (traced) Multivibrator Output Voltage Waveform

VOLTAGE-0.5v/cm
TIME-2u sec/cm

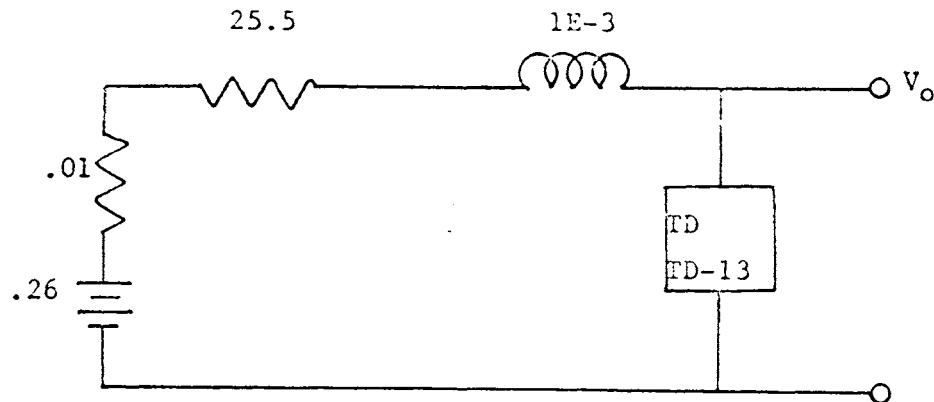


Figure 12 Astable Multivibrator

In the operation of the astable multivibrator the output voltage is zero volts to start out. It stays low until this tunnel diode voltage reaches peak voltage (V_p) then the output voltage goes straight up past valley voltage (V_v) due to inductor action. The voltage stays high until it has decayed to V_v then the voltage drops down to zero and it repeats. The waveform for this circuit output voltage shown on Photograph 4.

The ECAP data for Model 1 is shown in TABLE IV. The output waveform for the oscillator circuit, the voltage versus time at node 6, is shown in Figure 13.

The output waveform in Figure 13 approximates the actual device output voltage at the beginning but failed to go into oscillation.

The ECAP data for Model 2 is shown in TABLE V. The output waveform for the oscillator circuit, the voltage versus time at node 6 is shown in Figure 14.

TABLE IV Model 1 Oscillator ECAP Data

Transient Analysis	
B1	N(1,2), R=(10E7,0,36)
B2	N(2,6), G=(0.154,0.058), E=(0,-0.355), I=(0,-0.00095)
B3	N(2,6), R=10E8
B4	N(2,3), R=10E8
B5	N(3,6), R=0.001, E=-0.065
B6	N(2,6), R=10E8, E=0.355
B7	N(2,6), C=27E-12
B8	N(4,1), L=0.8E-9
B9	N(2,3), R=10E8
B10	N(4,0), R=22
B11	N(5,4), R=301
B12	N(0,5), R=0.1, E=5.9
B13	N(4,6), C=0.0005E-6
B14	N(6,0), C=0.0005E-6
B15	N(6,0), L=1E-3
T1	B(9,2), GM=(0,0.185)
T2	B(4,3), GM=(0,-0.185)
S1	B=1, (1), OFF
S2	B=5, (3,4), OFF
S3	B=6, (2,9), OFF

The output waveform of Figure 14 approximates the actual device output until the first diode switch tries to turn on at peak voltage (V_p). Then the switch oscillates for the remainder of the test.

The ECAP data for Model 3 is shown in TABLE VI. The output waveform for the oscillator circuit, voltage versus time at node 10, is shown in Figure 15.

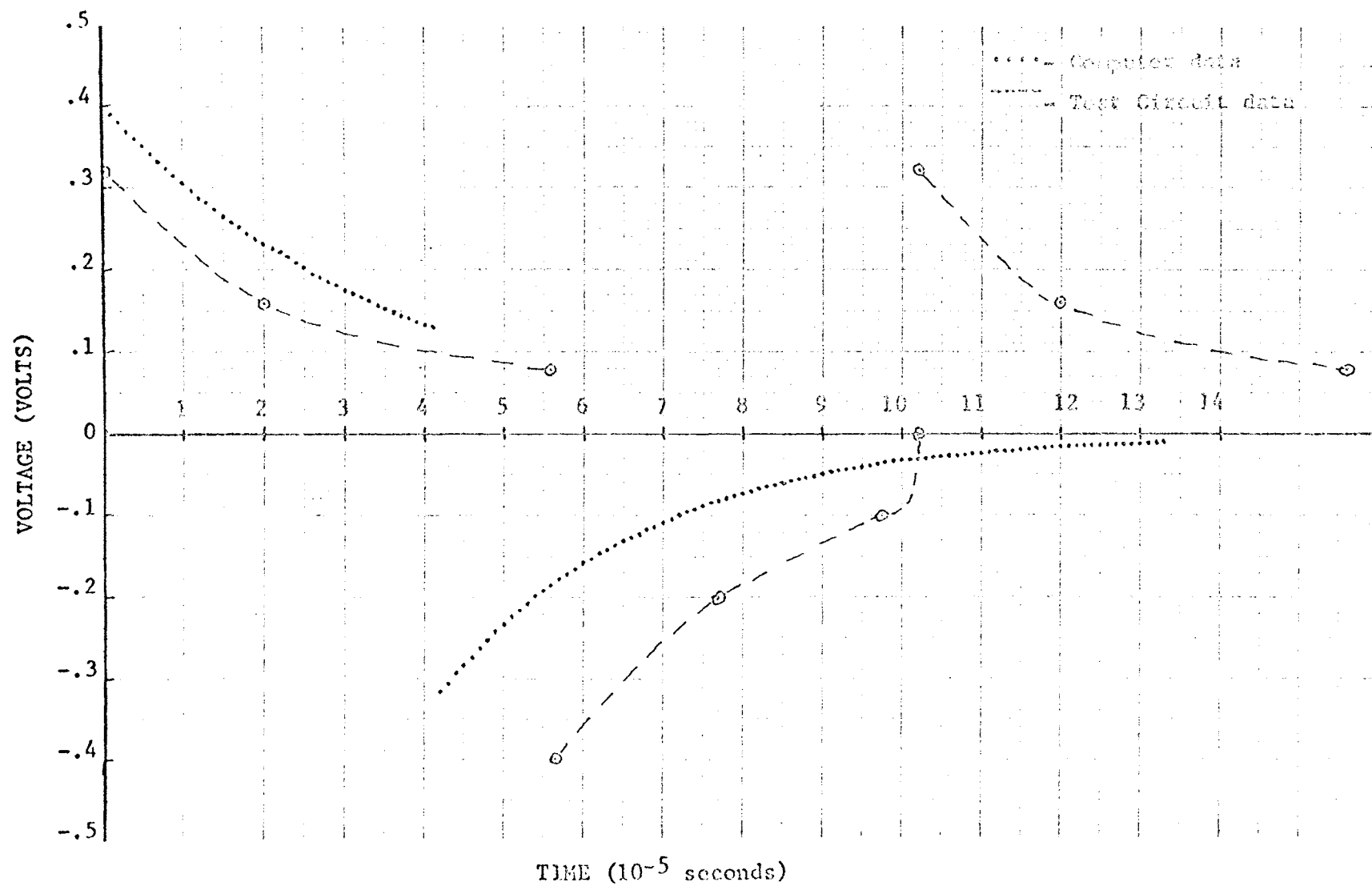


Figure 13 Model 1 Oscillator Output Waveform

TABLE V Model 2 Oscillator ECAP Data

Transient Analysis	
B1	N(1,2), R=(10E7,0.36)
B2	N(2,6), G=(0.161,1E-8)
B3	N(2,6), R=10E8, E=-0.0618
B4	N(2,3), R=10E8
B5	N(3,6), R=0.001, E=-0.0682
B6	N(2,6), R=10E8
B7	N(2,4), R=10E8
B8	N(4,6), R=0.001, E=-0.249
B9	N(2,6), R=10E8, I=(0,0.00905)
B10	N(2,6), G=(1E-8,0.0887), E=-0.408
B11	N(2,6), C=27E-12
B12	N(5,1), L=0.8E-9
B13	N(2,3), R=10E8
B14	N(7,5), R=301
B15	N(5,0), R=22
B16	N(0,7), R=0.1, E=5.6
B17	N(5,6), C=0.0005E-6
B18	N(6,0), C=0.0005E-6
B19	N(6,0), L=1E-3
T1	B(4,6), GM=(0,-0.0492)
T2	B(13,9), GM=(0,0.0492)
S1	B=1, (1), OFF
S2	B=3, (2,3), OFF
S3	B=5, (4,6), OFF
S4	B=8, (9,13), OFF
S5	B=10, (10), OFF

The output waveform in Figure 15 approximates the actual circuit waveform. The difference in amplitude and frequency is due to the different source voltage used in the ECAP model and the actual circuit.

The ECAP data for Model 1 is shown in TABLE VII. The output waveform for the multivibrator circuit, voltage versus time at node 6 is shown in Figure 16.

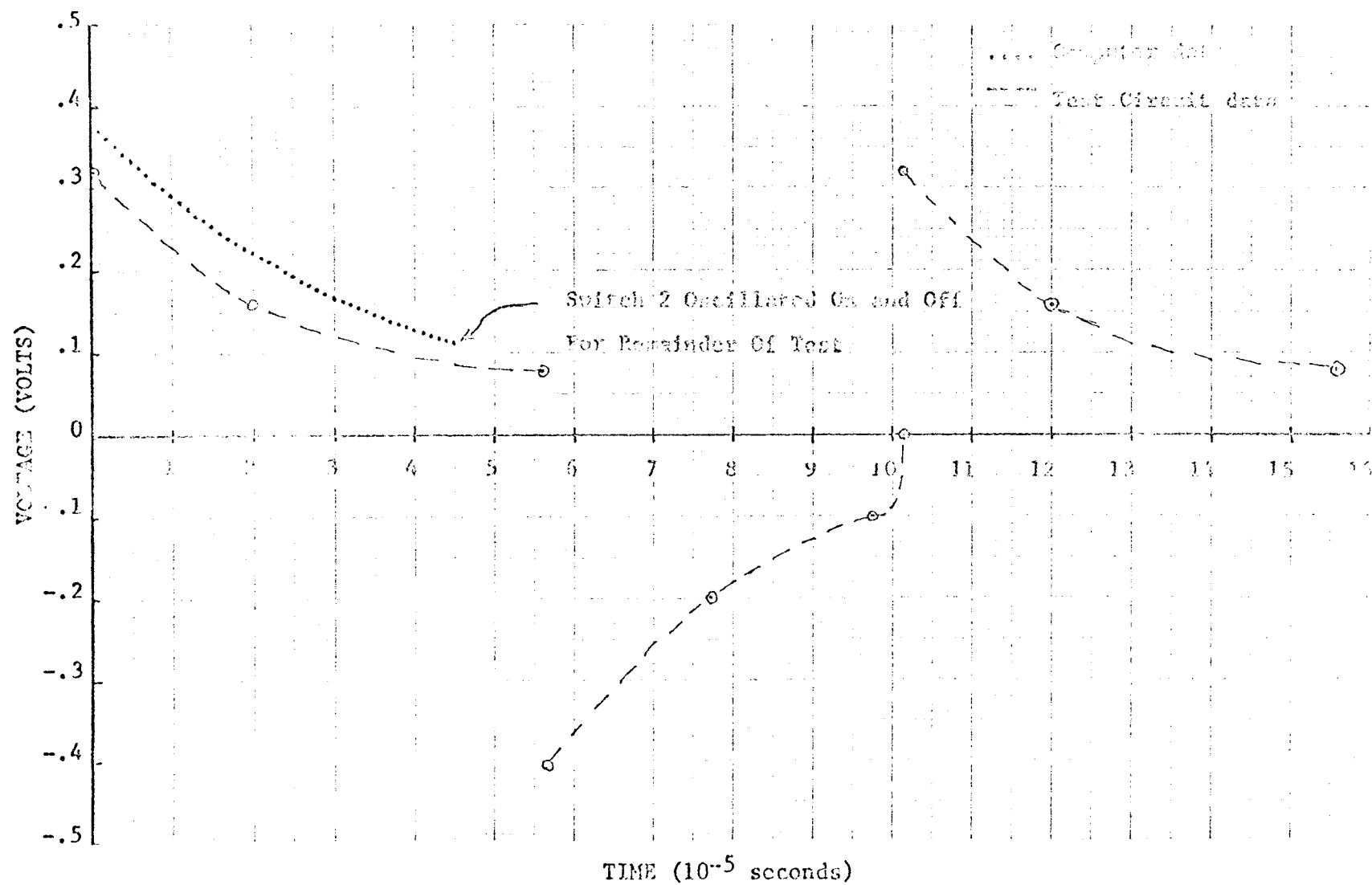


Figure 14 Model 2 Oscillator Output Waveform

TABLE VI Model 3 Oscillator ECAP Data

Transient Analysis	
B1	N(1,2), L=0.8E-9
B2	N(2,3), R=0.36
B3	N(3,10), G=0.154
B4	N(3,0), R=10E8, E=(-0.355,0)
B5	N(3,0), R=10E8, E=(-0.065,0)
B6	N(3,10), C=27E-12
B7	N(3,10), R=10E8, E=-0.355
B8	N(3,0), R=10E8, E=(-0.408,0)
B9	N(3,8), R=(0.01,10E8), E=(0,-0.45)
B10	N(3,10), C=2E-12
B11	N(10,4), R=(10,10E8), E=(1.5,0)
B12	N(4,5), R=(10E8,0.1)
B13	N(5,6), R=(0.1,10E8)
B14	N(7,6), R=(100,0.01)
B15	N(9,7), R=(10E8,0.01)
B16	N(10,9), R=(10E8,10), E=(0,0.875)
B17	N(6,10), C=0.05E-6
B18	N(6,10), G=0.308
B19	N(1,0), R=22
B20	N(11,1), R=301
B21	N(0,11), R=0.1, E-5.9
B22	N(1,10), C=0.0005E-6
B23	N(10,0), C=0.0005E-6
B24	N(10,0), L=1E-3
T1	B(18,3), BETA=(0,-0.8)
S1	B=5, (3,5,12,18), OFF
S2	B=4, (4,11,13), OFF
S3	B=10, (9,16), ON
S4	B=8, (8,15), OFF
S5	B=7, (14), OFF

The output waveform in Figure 16 approximates the actual device output voltage very closely.

The ECAP data for Model 2 is shown in TABLE VIII. The output waveform for the multivibrator, voltage versus time at node 5 is shown in Figure 17.

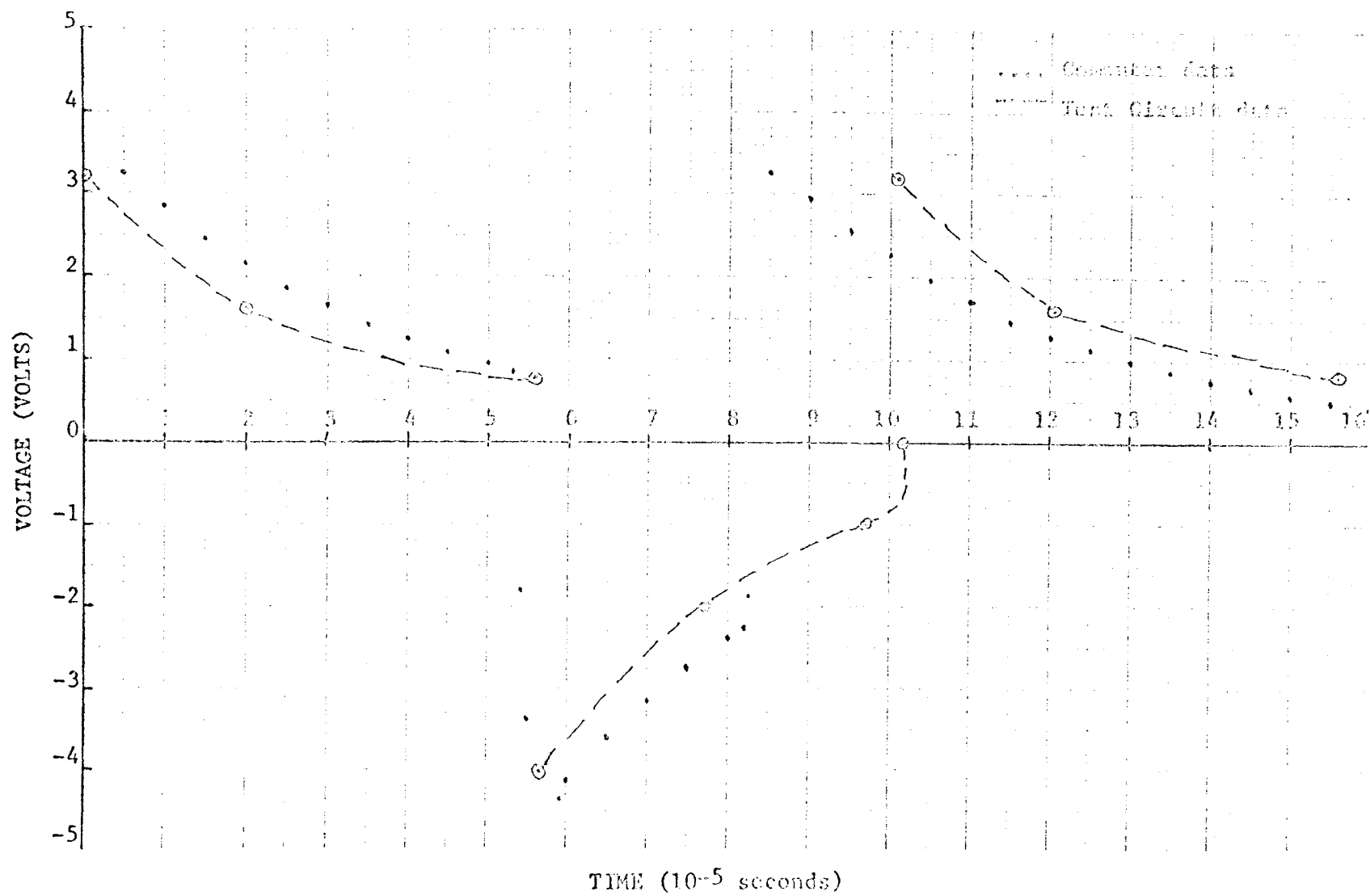


Figure 15 Model 3 Oscillator Output Waveform

TABLE VII Model 1 Multivibrator ECAP Data

Transient Analysis

B1 N(1,2), R=(10E7,1.7)
 B2 N(2,0), G=(0.0154,0.0058), E=(0,-0.355), I=(0,-0.000095)
 B3 N(2,0), R=10E8
 B4 N(2,3), R=10E8
 B5 N(3,0), R=0.001, E=-0.065
 B6 N(2,0), R=10E8, E=-0.355
 B7 N(2,0), C=3.5E-12
 B8 N(4,1), L=0.8E-9
 B9 N(2,3), R=10E8
 B10 N(5,4), L=1E-3
 B11 N(6,5), R=25.5
 B12 N(0,6), R=0.01, E=0.26
 T1 B(9,2), GM=(0,0.0185)
 T2 B(4,3), GM=(0,-0.0185)
 S1 B=1, (1), OFF
 S2 B=5, (3,4), OFF
 S3 B=6, (2,9), OFF

TABLE VIII Model 2 Multivibrator ECAP Data

Transient Analysis

B1 N(1,2), R=(10E7,1.7)
 B2 N(2,0), G=(0.0161,1E-8)
 B3 N(2,0), R=10E8, E=-0.0618, I=(0,-0.001)
 B4 N(2,3), R=10E8
 B5 N(3,0), R=0.001, E=-0.0682
 B6 N(2,0), R=10E8
 B7 N(2,4), R=10E8
 B8 N(4,0), R=0.001, E=-0.249
 B9 N(2,0), R=10E8, I=(0,0.000905)
 B10 N(2,0), G=(1E-8,0.00887), E=-0.408
 B11 N(2,0), C=3.5E-12
 B12 N(5,1), L=0.8E-9
 B13 N(2,3), R=10E8
 B14 N(6,5), L=1E-3
 B15 N(7,6), R=25.5
 B16 N(1,7), R=0.01, E=0.26
 T1 B(4,6), GM=(0,-0.00492)
 T2 B(13,9), GM=(0,0.00492)
 S1 B=1, (1), OFF
 S2 B=3, (2,3), OFF
 S3 B=5, (4,6), OFF
 S4 B=8, (9,13), OFF
 S5 B=10, (10), OFF

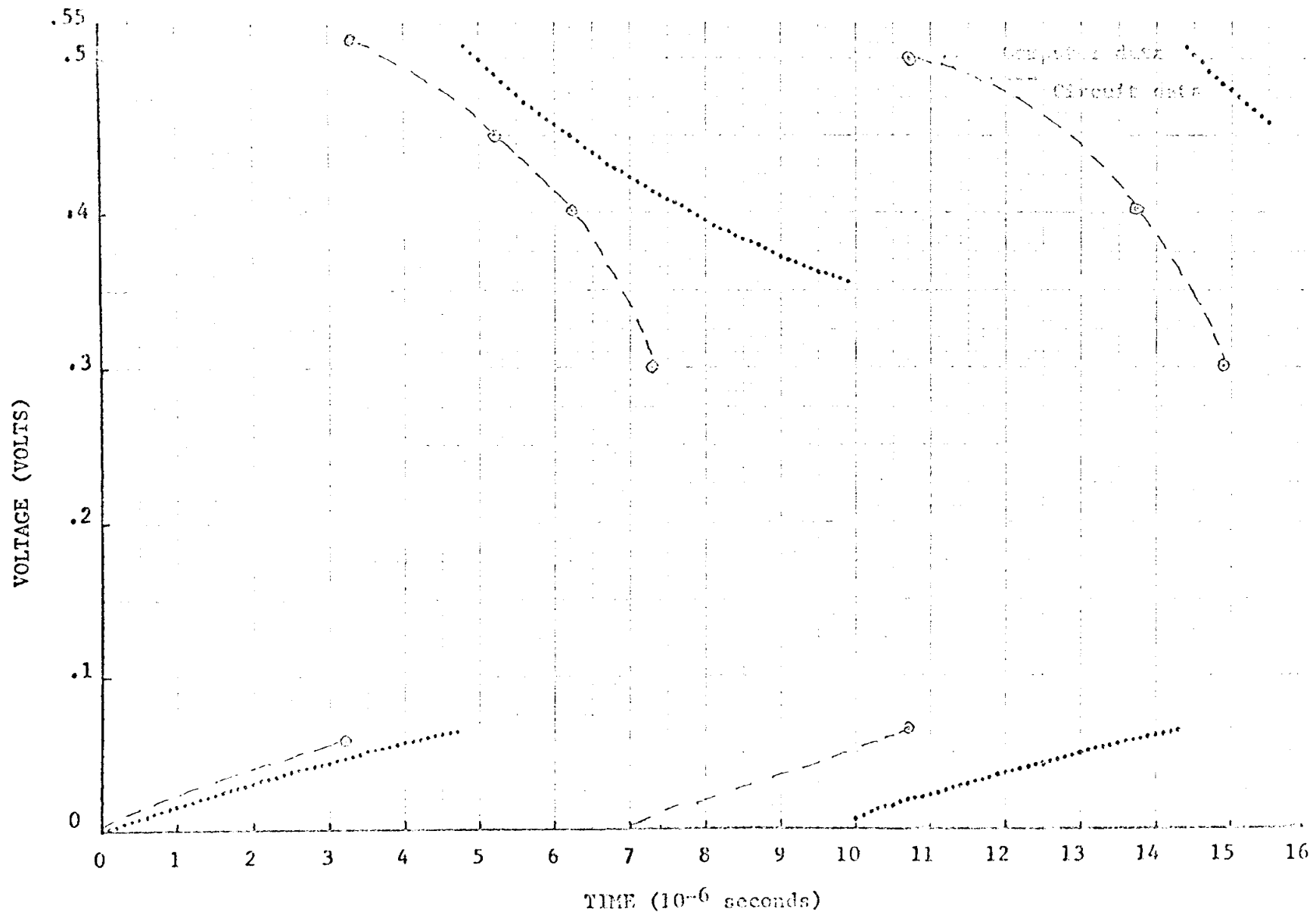


Figure 35 Model 1 Multivibrator Output Waveform

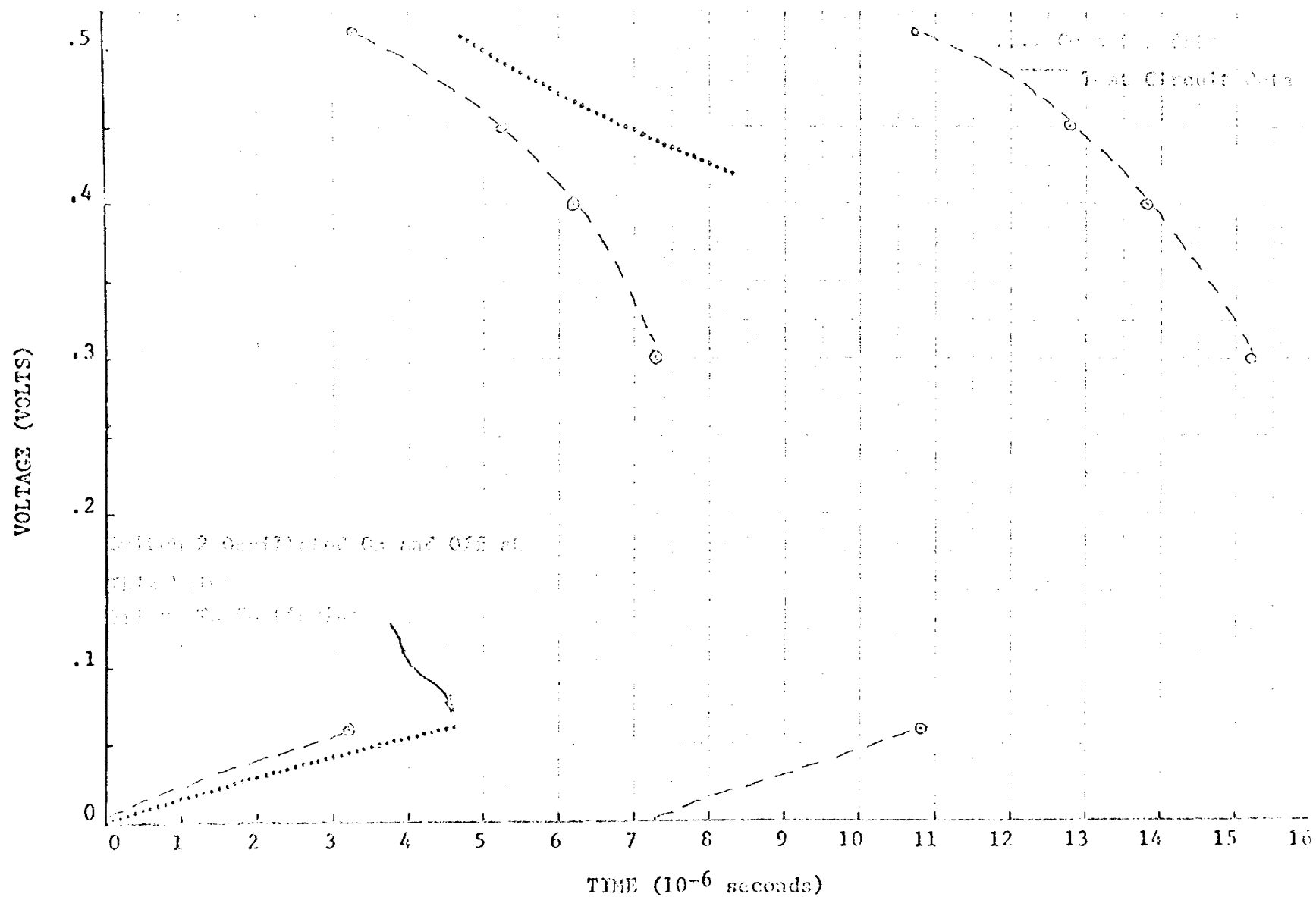


Figure 17 Model 2 Multivibrator Output Waveform

The output waveform in Figure 17 approximates the actual device output voltage, however, like Model 2 on the oscillator circuit, the first switch at tunnel diode peak voltage oscillated for approximately half of the program before continuing.

IV. CONCLUSIONS

These three models are similar in that they all change current levels to simulate the tunnel diode curve. They are different in complexity and also in the type of elements used to change the current.

Model 1, the three section piecewise-linear model, is the simplest of the three. The element used in generating the current-voltage curve is the dependent current source. The curve is generated by switching in or out the proper dependent current element. The data plotted in Figure 4 shows that the model displays the negative resistance region and accurately follows specified path for increasing and decreasing voltage.

Model 2, the five section piecewise-linear model, is similar to Model 1 using straight lines, although, it more closely simulated the actual tunnel diode current-voltage characteristic. Model 2 switches both dependent and independent current sources in or out of the circuit to generate its current-voltage curve. The data plotted in Figure 7 shows that the model duplicates the desired curve for both increasing and decreasing voltages.

Model 3 has a smooth current-voltage curve as opposed to straight lines of Models 1 and 2. This model switches in and out current generated from an RC circuit. The data plotted in Figure 10 shows the model as simulating a portion of the desired curve for voltage up to valley voltage then the model deviates from the desired curve, although, it still looks like a tunnel

diode for increasing voltage. The model can simulate a device where the decreasing voltage is not used. The characteristic for decreasing voltage looks like a tunnel diode curve but again differs considerably from the desired curve. The reason for the difference is due to the method of selecting the parameters. On this model it was done by a trial and error method. Parameter selection is covered in more detail in Appendix II.

To verify the operation of the models in circuits, data was taken on Models 1, 2 and 3 in a relaxation oscillator and Models 1 and 2 in an astable multivibrator. Due to the method of switching in and out the current in Model 1 and 2, the time step must be selected in relationship to the smallest time constant of the circuit. If the time step is too large the switch will oscillate. This problem existed on Models 1 and 2 until the time step was selected in the range of $1\text{E}-9$ to $1\text{E}-11$. This greatly extends the computer time requiring an hour to run a program of 10-100 microseconds. Model 3 using current generated in an RC circuit does not have the same problem at the switches, since the nature of RC circuits is a more gradual change, this allows Model 3 to use a large time step, in the range of $2.5\text{E}-6$ and thereby reduce the computer time required.

The data plotted for Model 1 in the oscillator circuit, Figure 13 shows the output voltage as starting as the actual circuit Photograph 3 however, it does not go into oscillation. The voltage used in the ECAP program is 5.9 volts which is the

actual circuit was at upper threshold of oscillation. The model seems to be performing as expected, and if the circuit was rerun using a lower voltage such as 5.6 or 5.3 volts the output voltage would oscillate similar to the actual device voltage.

The data plotted in Figure 16 for Model 1 in the multivibrator circuit shows the model performing as expected. Comparing the plotted results to Photograph 4, Model 1 does simulate the tunnel diode, in the multivibrator circuit.

The data plotted in Figure 14 for Model 2 in the oscillator circuit shows that the model goes into switch oscillation at tunnel diode peak voltage the first switching of a current element, and doesn't get past the switch. The data plotted for Model 2 in multivibrator circuit shown in Figure 17 shows the same problem as the oscillation circuit. In the multivibrator circuit the switch S2 oscillated until the current in the tunnel diode increased enough to supply the current source and the remaining elements. Then the program proceeded. After that point the model simulates the first portion of the actual waveform in Photograph 4.

When the switch S2 is turned on an independent current source is turned on to maintain constant level of current. The current level of the independent current source is the level of the tunnel diode input current at the time of the switching. The current is being divided with other elements. The current available from the voltage source is less than required by the current source and with the series inductance in the circuit, the capacitor is the only element that the current source can draw the current

required. The capacitor discharges and turns off the switch. Then voltage level increases and the switch turns on again. If the inductor is removed from the circuit the current source could receive all its current from the voltage source and should not get switch oscillation.

Model 3 was only tested in the oscillator circuit because the model was only set up for the TD-19 circuit. The method of determining the parameters of Model 3 does not allow easy conversion to a new diode. The data plotted in Figure 15 shows that that circuit will oscillate and represents the actual diode as shown in Photograph 3. Differences between the two curves is due to a difference circuit voltage used on the circuit.

Model 1 simulates the tunnel diode in the circuits tested. The model is simple although, it required considerable computer time to run each circuit.

Model 2 did not give acceptable results, although, with small modifications it could operate as intended. One possible modification is to remove the series inductor (L_s) from the circuit.

Model 3 adequately simulated a tunnel diode in the oscillator circuit. The computer time required is considerably less than the other two models. This is offset by the complexity of the model and the method used to select the parameters. The trade off to be considered when selecting the model in parameter calculating time versus computer time.

APPENDIX I

SUMMARY OF MODELING OF ACTIVE DEVICES FOR COMPUTER-AIDED CIRCUIT DESIGN

Computer-Aided Circuit Analysis is one of the fast expanding uses of the computers of today. Many programs have been written to analyze or design electronic circuits. Many were designed for one specific purpose; for example, Low-Pass Elliptic Filter^[3], Band Pass Ladder Crystal Filter Design^[4], Poles and Zeros of Amplifier Transfer Functions^[4,11], Flip Flop Worst Case Design^[3], Inverter Worst Case Design^[3], Environmental Resistance Inherent in Equipment^[4] and numerous others.

Some programs of a more general nature have been developed that can be used to analyze many kinds of circuits, some such programs are Transistor Circuit Analysis (NET-1)^[4,10], System for Circuit Evaluation and Prediction of Transient Radiation Effect (SCOPE)^[13], Electronic Circuit Analysis of Electronic Circuits (CIRCUS)^[2].

All of the programs, both specific and general, must in some way be able to simulate mathematically the various passive and active components of the circuitry being analyzed. The accuracy of the results of any of these programs and the efficient use of computer time depends largely on the adequacy of the models used.

Modeling may be defined as the process of formulating a mathematical description of the behavior of a physical device. The models are classed as linear or non-linear depending on the type of differential equations which describe the current-voltage characteristics. The models for resistors, capacitors, inductors, voltage sources, and current sources are generally included as

stored models of the programs. Models for diodes, transistors and other active devices are non-linear type. NET-1, SCEPTRE and CIRCUS have some of these models stored in their programs. Some programs, ECAP in particular requires the user to supply the models. ECAP, while not handling the non-linear models, can still approximate non-linear devices with piecewise-linear models. Regardless of which program is used, the models must be developed to simulate these devices. A number of models have been developed for the diode. The primary difference in these various models is the different elements used to simulate the device and the parameters used for these various elements. These differences arise from linearity or non-linearity of the model and the accuracy required. Diode current-voltage curves simulated by various models are shown in Figure I-1.

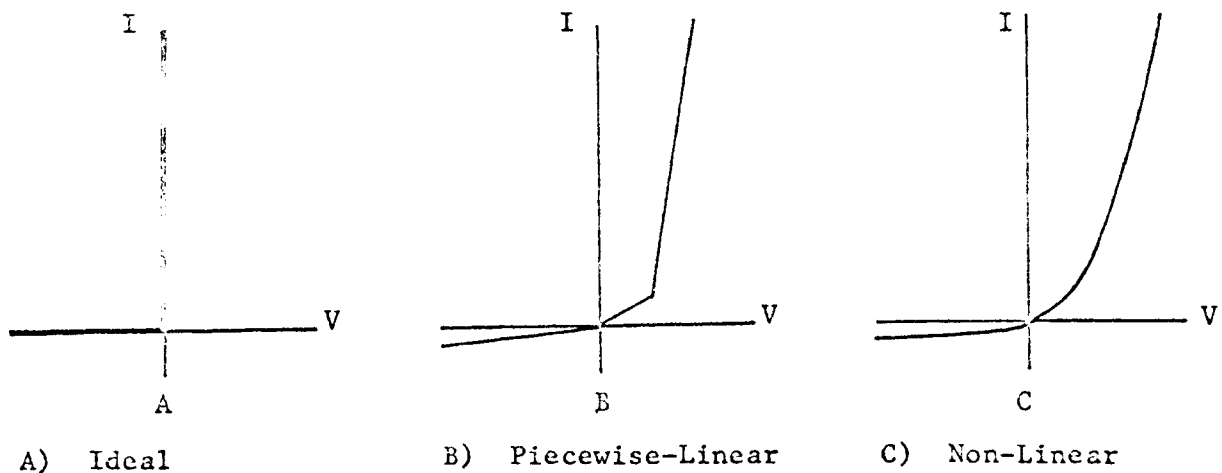


Figure I-1 Diode Current-Voltage Characteristic

The simple linear switching diode model[6] Figure I-2A with large resistance when the current is in the reverse direction and small resistance when the current is in the forward direction approximates the current-voltage curve of Figure I-1A. The more complex model[1] Figure I-2B which takes into account transition capacitance diffusion capacitance, bulk, and leakage resistances, and current source approximates the current-voltage curve of Figure I-1B or I-1C. This model can be linear or non-linear depending on the values of the elements of the model. The more complex the model the more parameters must be supplied to simulate a device.

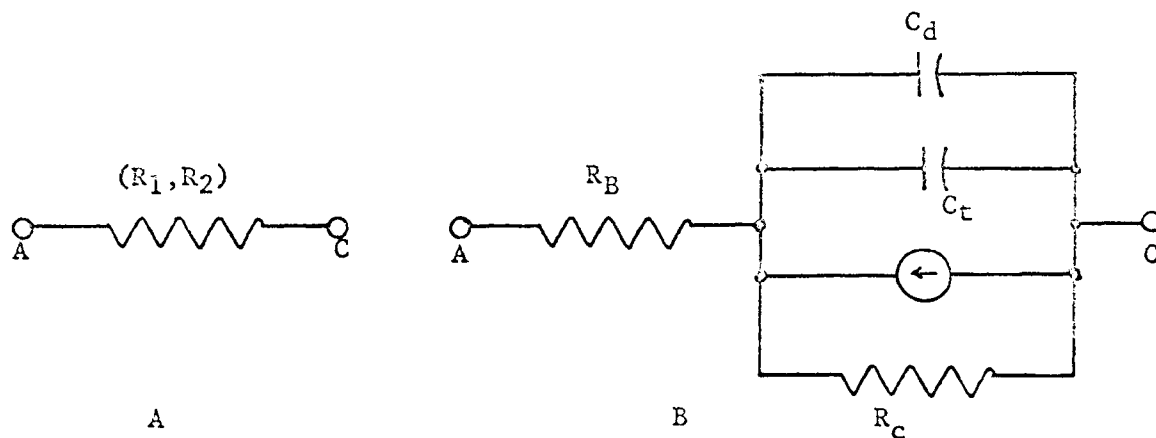


Figure I-2 Diode Models

The number and type of elements used in a model is a function of the approach taken to simulate the current-voltage relationship. One approach is to use conventional elements to develop the required current-voltage curve without using the device parameters. An alternate approach is to use conventional elements to develop the required current-voltage curve but use the device parameters plus

additional measurements. This approach is used with the Ebers-Moll model[4] Figure I-3.

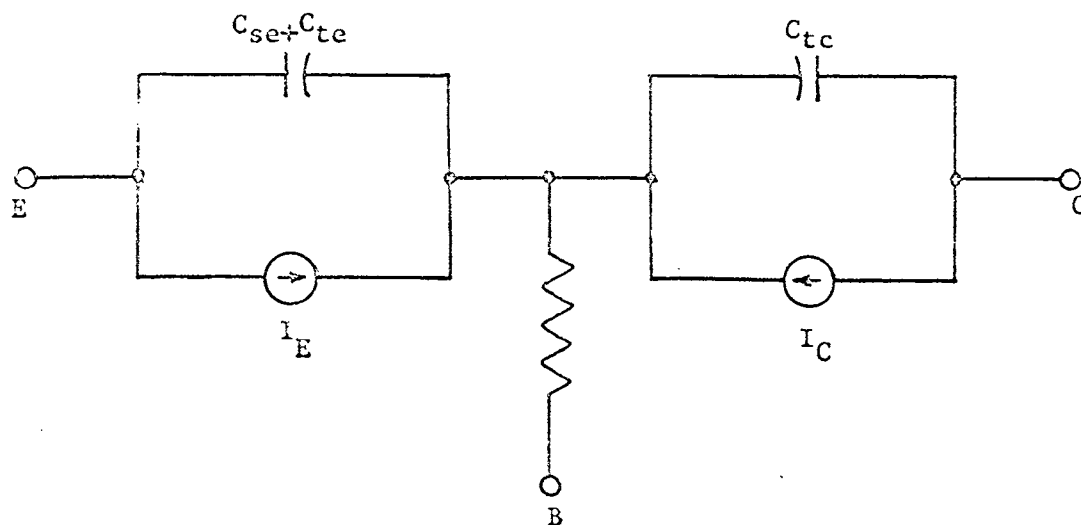


Figure I-3 Ebers-Moll Model

A third approach used in the development of the Beaufoy-Sparks Charge Control model[4] Figure I-4 and the Linvill Lumped model[8,9,14] Figure I-5 is to approximate the current-voltage curve by using conventional elements and by creating new elements as required. The new elements are used to simulate an internal physical phenomenon. Beaufoy-Sparks Charge Control model introduced the base store S_b element. Linvill Lumped model introduced three new elements, storance S_e , diffusance π_d and combinance W_e . The Linvill model most closely represents the physical device phenomenon, however the Ebers-Moll model is used most widely because no new circuit elements are required. This is an advantage since the element values can be determined by measuring a typical

unit or assured from the manufacturer's sheet.

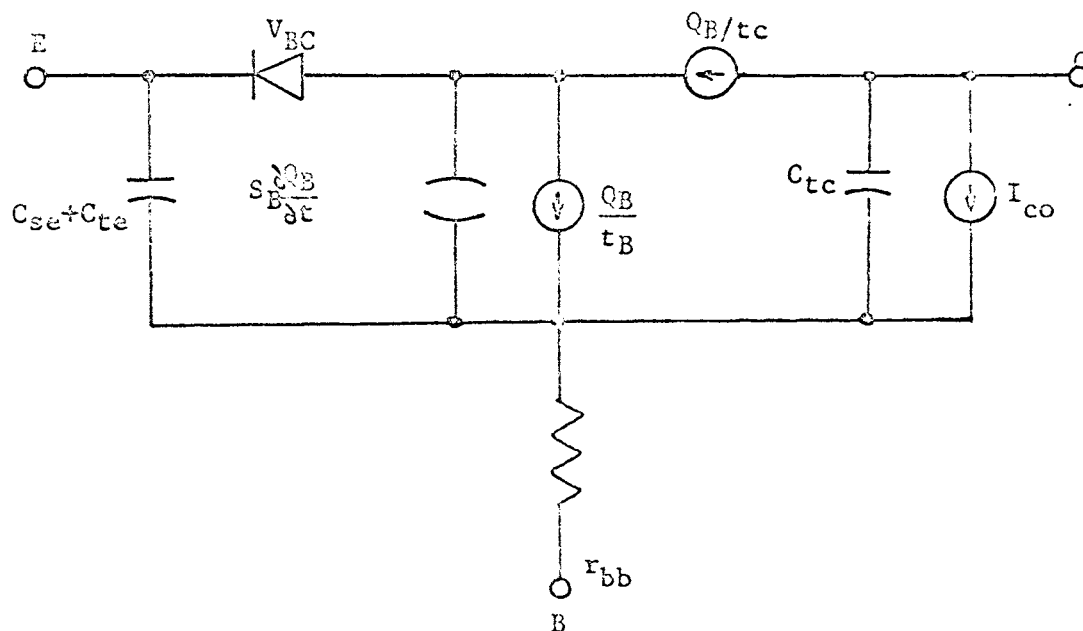


Figure I-4 Beaufoy-Sparks Charge Control Model

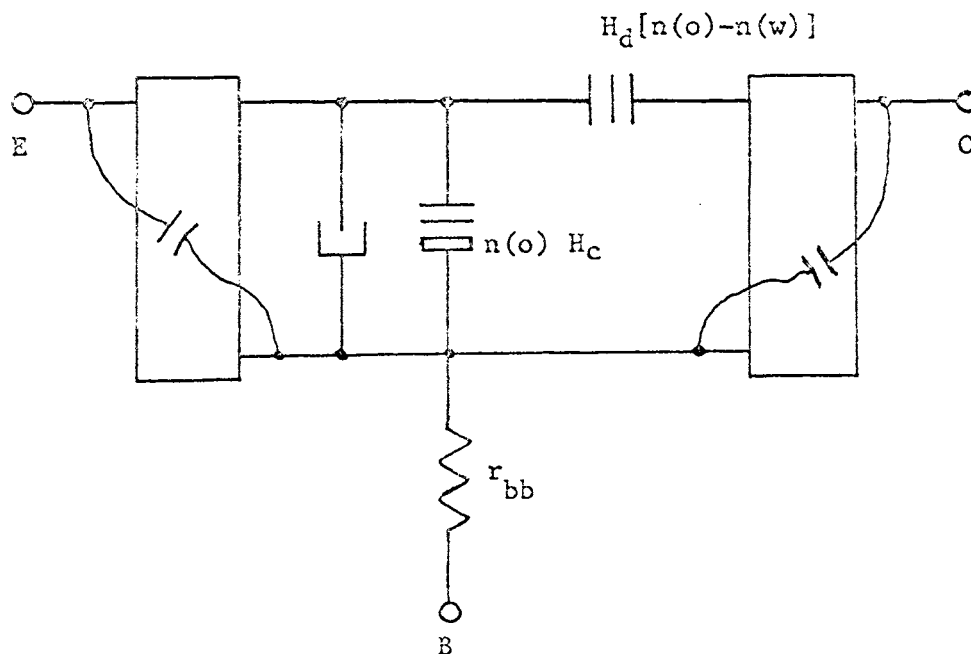


Figure I-5 Linvill Lumped Model

Work has been done on a Zener Diode model[1] Figure I-6 by modifying Ebers-Moll diode topology of Figure I-2B. This model can be linear or non-linear depending on the values of I_1 and I_2 .

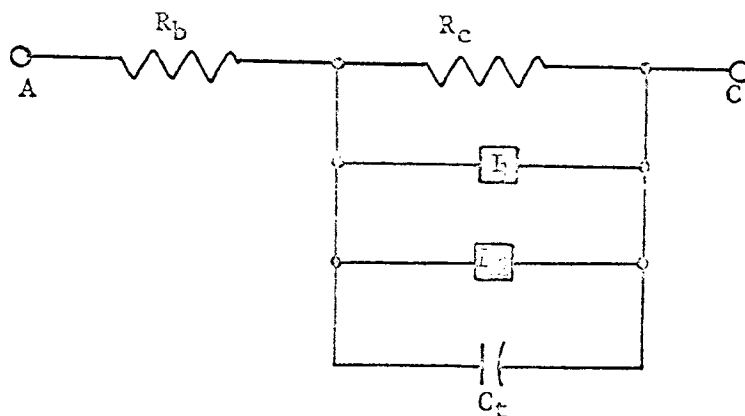


Figure I-6 Zener Diode Model

Some work has been done with negative resistance devices, Daniels[1] put forth several curve fitting methods for tunnel diodes by fitting the entire function with $I(v) = A_0 e^{-ab} + B(e^{b_1 v} - e^{b_2 v}) + C(e^{c v} - 1)$. This equation is the sum of the tunneling current, the diffusion current, and the excess current, respectively. Another method of representing the V-I characteristic is to divide it into several zones and fitting the curve with a polynomial of the form $I(v) = A_0 + A_1 v^2 + A_2 v = \dots + A_n v^n$. The $A_0, A_1, A_2, \dots, A_n$ are obtained from measured data.

R. W. Jensen and M.D. Liebermann[7] in their book IBM Electronic Circuit Analysis Program Techniques and Applications show a turned diode model for ECAP. See Figure I-7.

The model uses negative resistors to provide the negative slope. The capacitor is added to prevent the model from locking

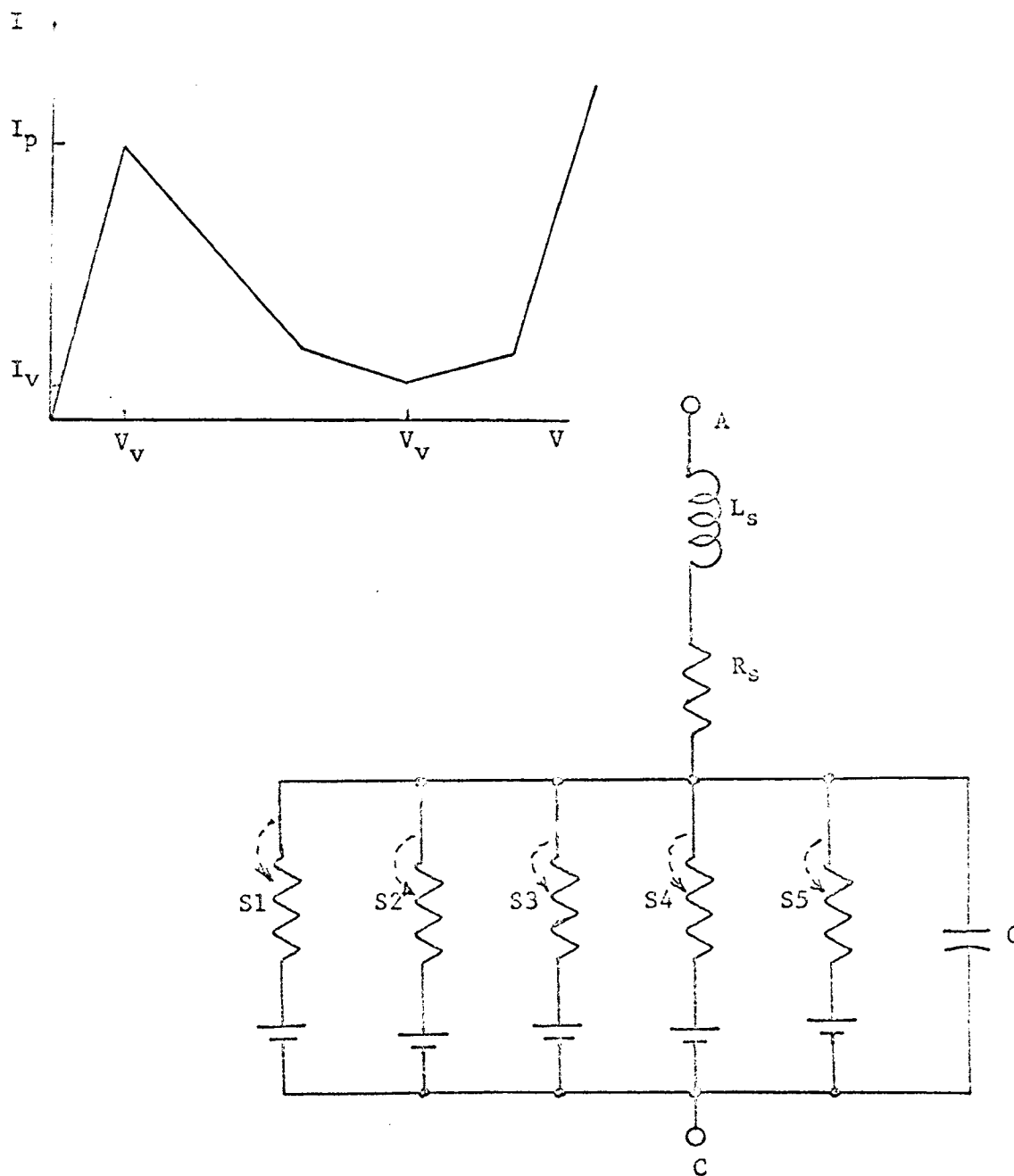


Figure I-7 Tunnel Diode Model

up. Lock up can occur when the model is switching to the negative resistance at V_p , and decreasing voltage causes the current-voltage curve to follow a decreasing voltage and increasing current path instead of the desired curve. The capacitor pre-

vents the voltage from decreasing at V_p point. This condition requires that care be taken in selecting the value for shunt capacitor.

An additional restriction is the selection of the time-step. The parasitic elements are very important when considering the transient response of the model. The time-step must be in the range of the parasitic element time constant.

REFERENCES

- [1] DANIEL, M.E. (1967) Development of Mathematical Models of Semiconductor Devices for Computer-Aided Circuit Design, Proceeding of IEEE, vol. 55 no. 11, November, p. 1913-1920.
- [2] Digital Computer Program for Transient Analysis of Electronics Circuit (CIRCUS) (346-1) User's Guide, Seattle, Washington, Boeing Company, 1967.
- [3] FALK, H. (1964) Computer Programs for Circuit Design, Electro-Technology, vol. 73 no. 3, March, p. 101-103, 162, 164.
- [4] FALK, H. (1966) Computer Programs for Circuit Design, Electro-Technology, vol. 77 no. 6, June, p. 54-57.
- [5] HARBOUR, C.O. (1967) Computer-Aided Design Part 5: Doing a Model Job, Electronics, vol. 40 no. 2, January 23, p. 82-87.
- [6] The 1620 Electronic Circuit Analysis Program (ECAP) (1620-EE-02K) User's Manual, White Plains, N.Y., International Business Machines Corp., 1965.
- [7] JENSEN, R.W., and LIEBERMAN, M.D. (1966) IBM Electronic Circuit Analysis Program Techniques and Applications, Englewood Cliffs, New Jersey, Prentice-Hall, Inc., p. 106-154.
- [8] LINVILL, John G. (1958) Lumped Models of Transistors and Diodes, Proceeding of the IRE, vol. 46 no. 6, June, p. 1141-1152.
- [9] LINVILL, John G. (1963) Models of Transistors and Diodes, New York, McGraw-Hill, Inc.
- [10] MALMBERG, A.F., CORNWELL, F.L. and KOEHLER, F.N. (1964) NEF-1 Network Analysis Program, Report No. LA-3119, Los Alamos Scientific Laboratory, 7090/94 Version, August.
- [11] RIPS, E.M. (1967) Calculating Amplifier Poles and Zeros with Digital Computer, EEE, vol. 15 no. 2, February, p. 94-100.

- [12] Revised SCEPTRE User's Manual: Vol, 1, (AFWL-TR-67-124),
Kirtland Air Force Base, New Mexico, International
, Business Machines Corp., April 1968.
- [13] SCHEERER, W.G. (1968) Selecting Device Models for Computer-
Aided Design, Electro-Technology, vol. 81,
no. 55, May, p. 43-48

APPENDIX II

ANALYSIS, CALCULATION AND SELECTION
OF PARAMETER FOR TUNNEL DIODE MODELS

All of the models have several elements, large resistance 10^8 ohms, and small resistance 0.001 ohm, which are used as current sensing elements and are the same for any tunnel diode being represented. Also common to all models is L_s , R_s and C_1 , series inductance, series resistance and terminal capacitance respectively. The value for these elements can be obtained from the manufacturer's data sheet. See TABLE II-1. Figure II-1 shows relationship of parameters in TABLE I to current-voltage curve.

TABLE II-1
DATA FROM G.E. DATA SHEET

<u>Parameter</u>	<u>Symbol</u>	<u>TD-19</u>	<u>TD-13</u>
Peak Point Current	I_p	10.00 ma	1ma
Valley Point Current	I_v	.95 ma	.095 ma
Peak Point Voltage	V_p	65 mv	65 mv
Valley Point Voltage	V_v	355 mv	355 mv
Reverse Voltage ($I_R=I_p$)	V_R	20 mv	20 mv
Forward Voltage ($I_F=I_p$)	V_{fp}	510 mv	510 mv
Series Inductance	L_s	0.8 nh	0.8 nh
Series Resistance	R_s	0.36 ohms	1.7 ohms
Terminal Capacitance	C_1	27 pf	3.5 pf
Negative Terminal Conductance	$-G$	85×10^{-3} mho	8.5×10^{-3} mho

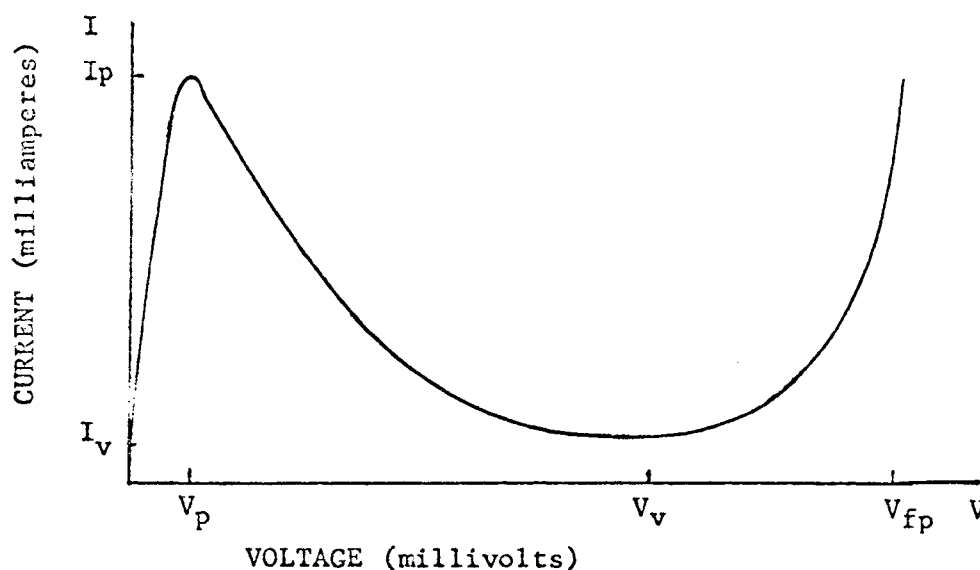


Figure II-1 Tunnel Diode Current-Voltage Characteristic

Model 1 shown in Figure II-2 is a three section piecewise-linear model. The elements simulate the three straight lines depending on the terminal voltage. S1 turns the diode off when the diode is back bias. When the voltage is between 0 and peak voltage the model consists of L_s , R_s in series with G_1 and C_1 in parallel. When looking at the current-voltage characteristic this becomes the slope associated with the line from (0,0) to (V_p, I_p) . When peak voltage level is reached, switch S2 is activated and turns on a dependent current in R_3 . The current source has a $-GM_1$ and is putting current into the model thereby reducing the diode current with increasing voltage. This is the negative resistance line and it consists of the sum of G_1 line and the $-GM_1$ line to give the desired negative resistance to the model. When valley voltage level

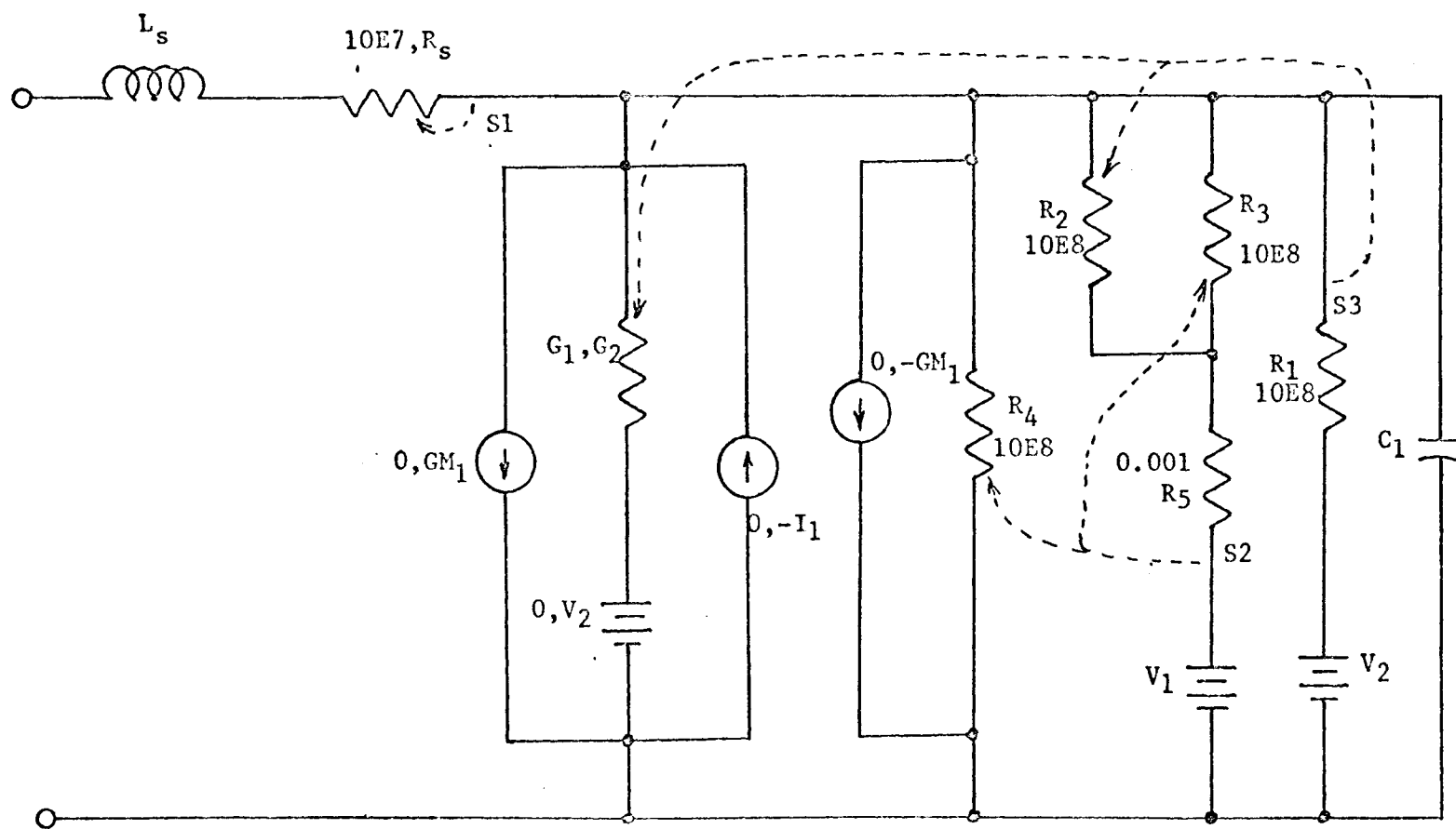


Figure II-2 Model 1

is reached, S3 switches G_1 to G_2 , turns on a controlled current source GM_1 controlled by R_2 to cancel the $-GM$. S3 also turns on I_1 to control the current level at V_v the point where the third section starts. For decreasing voltage the diode retraces the same path.

Model 1 shown in Figure II-2 has elements L_s , G_1 , G_2 , V_1 , V_2 , GM_1 , I_1 , and C_1 which must be specified from data of the particular tunnel diode.

Selecting values for these elements depend on how the current-voltage characteristic is to be approximated. Figure II-3 shows the tunnel diode current-voltage characteristic and three ways to select and approximation to the curves. Of the three shown, they all have about the same amount of error when compared with the actual model curve. The first curve using the (V_p, I_p) and (V_v, I_v) points was selected in this paper. Using this curve as the approximation V_1 and V_2 are V_p and V_v respectively.

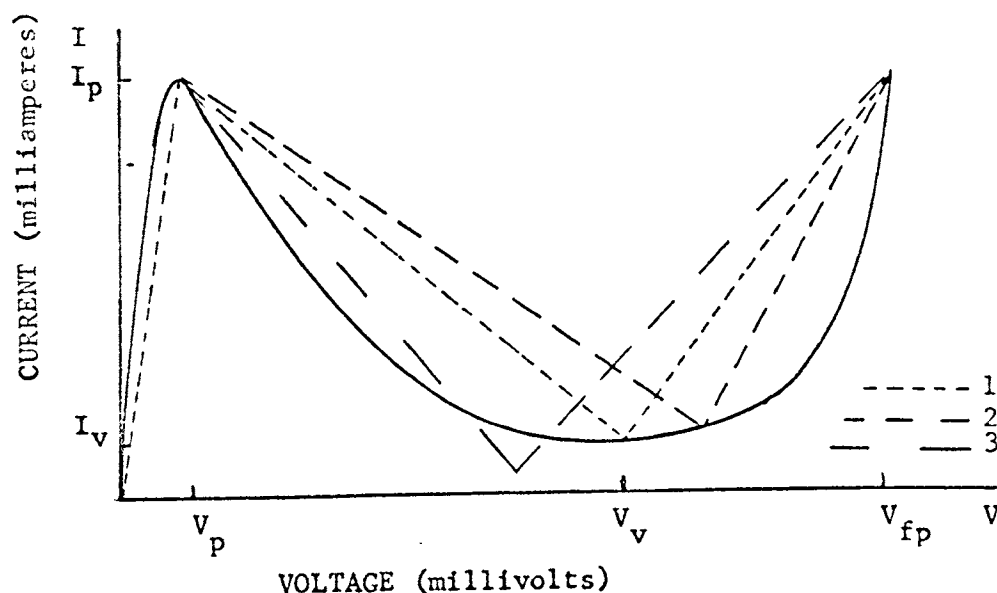


Figure II-3 Three Section Piecewise-Linear Current-Voltage Curve

$$V_1 = V_p$$

$$V_2 = V_v$$

G_1 , G_2 , GM_1 and I_1 are obtained from the following relationships:

$$GM_1 = \frac{V_v G_1 - I_v}{V_v - V_p}$$

$$I_1 = I_v$$

$$G_1 = \frac{I_p}{V_p}$$

$$G_2 = \frac{I_f - I_v}{V_f - V_v}$$

For $I_f = I_p$:

$$G_2 = \frac{I_p - I_v}{V_f - V_v}$$

The specific values for Model 1 representing TD-19 and TD-13 are shown in TABLE II-2.

TABLE II-2

MODEL 1 PARAMETER VALUES			
<u>Parameter</u>	<u>TD-19</u>	<u>TD-13</u>	
V_1	0.065	0.065	volts
V_2	0.355	0.355	volts
G_1	0.154	0.0154	mho
G_2	0.058	0.0058	mho
GM_1	0.185	0.0185	
I_1	0.00095	0.000095	amp

Model 2 shown in Figure II-4 is a five section piecewise-linear model. When the voltage is between 0 and the diode peak voltage, G_1 element provides the first line from 0 to V_1 . At V_1 the switch S_2 turns on. It changes G_1 to an open circuit and turns on an independent current source $-I_1$ which draws current from the device and maintains the current level constant at I_1 from V_1 to V_2 . At V_2 switch S_3 turns on a controlled current source $-GM_1$ which is controlled by R_4 . This source removes sufficient current to generate the negative resistance portion of the curve from V_2 to V_3 . At V_3 switch S_4 turns on a controlled current source GM_1 which is controlled by R_3 and cancel the effect of the $-GM_1$ of switch S_3 . S_4 also turns on an independent current source I_2 which supplies current to the device to maintain the current level constant at I_2 from V_3 to V_4 . At V_4 switch S_5 turns on and G_2 is then in the circuit and is the element which generates the line from V_4 to V_{fp} . For decreasing voltage the diode retraces the same path.

S_1 turns the diode on if the diode is forward bias and off if the diode is reverse bias.

The elements simulate the five straight lines depending on the terminal voltage.

Model 2 shown in Figure II-4 has elements L_s , C_1 , G_1 , G_2 , V_1 , V_2 , V_3 , V_4 , GM_1 , I_1 , and I_2 which must be specified from data of the particular device.

The selection of values for these elements depend on the

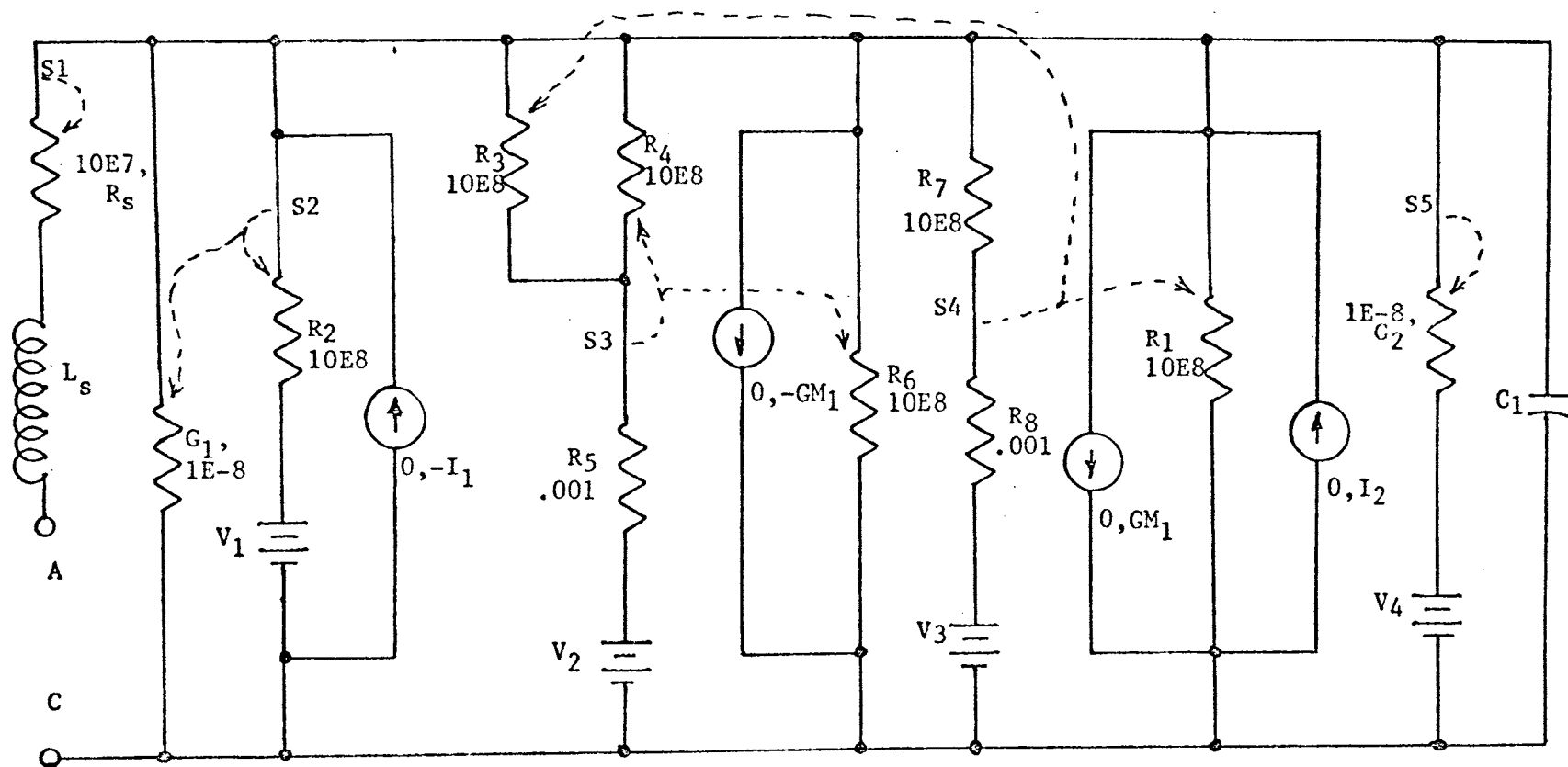


Figure II-4 Model 2

current-voltage characteristic shown in Figure II-5.

This curve is a better approximation to the actual device than the Model 1 curve. The voltage ratios selected are dependent on the shape of the current-voltage characteristic and for tunnel diodes with a curve proportioned differently, the voltage would be different.

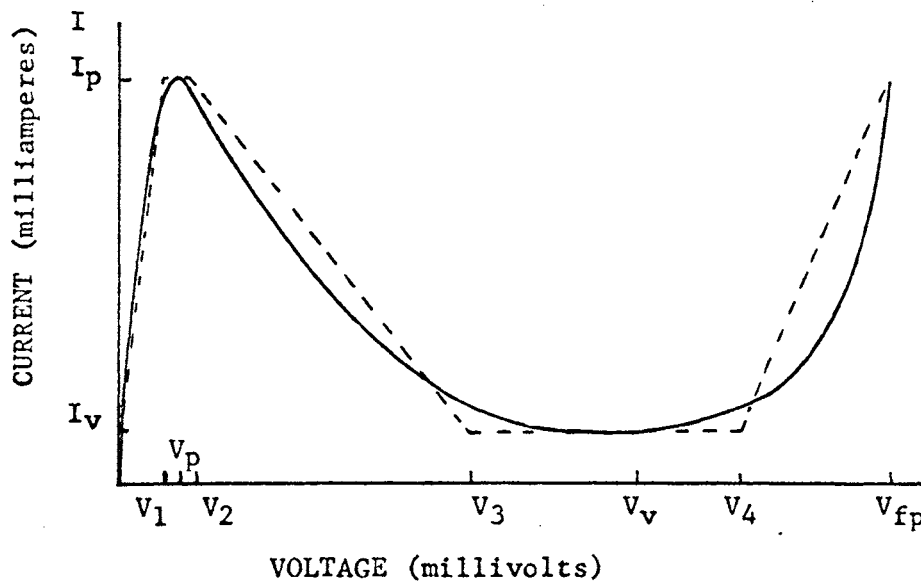


Figure II-5 Five Section Piecewise-Linear Current-Voltage Curve

The voltage V_1 , V_2 , V_3 and V_4 are the following:

$$V_1 = .95V_p$$

$$V_2 = 1.05V_p$$

$$V_3 = .70V_v$$

$$V_4 = 1.15V_v$$

G_1 , G_2 , G_M , I_1 and I_2 are obtained from the following relationship:

$$G_M = \frac{I_p - I_v}{V_3 - V_p}$$

$$I_1 = I_p$$

$$I_2 = I_p - I_v$$

$$G_1 = \frac{I_p}{V_1}$$

$$G_2 = \frac{I_f - I_v}{V_f - V_4}$$

For $I_f = I_p$:

$$G_2 = \frac{I_p - I_v}{V_f - V_4}$$

The specific values for Model 2 representing TD-19 and TD-13 are shown in TABLE II-3.

Model 3 shown in Figure II-6 is a smooth curve model. The elements simulate the model so there are no sharp corners. The curve, like the other models, is made up of pieces. The elements L_s in series R_s in parallel with G_1 and C_1 provide the waveform from 0 to V_p . At V_p , S_1 turns on a controlled current source $-BETA$ which is controlled by G_2 . S_1 also closes the open resistor R_6 to allow the capacitor C_2 to charge up and supply current to G_2 . This develops the negative resistance portion of the curve by subtracting $BETA$ times the G_2 current from the initial waveform, which continues from V_p to V_v . At V_v the switch S_2 turns on and opens resistor R_7 . This removes the voltage source from C_2 it

discharges, increasing current in G_1 and generating the portion of the curve that goes from V_v up. At the same time S_4 and S_5 have turned on setting up the circuitry, R_9 , R_{10} , R_{11} and 0.875 voltage generator, for decreasing voltage. S_4 shorts R_9 and S_5 shorts R_{10} . When the voltage starts down capacitor C_3 (also S_3) senses the change and R_{11} is reduced to 10 ohms. C_2 is charged up causing the current in G_1 to decrease and generate the curve down to V_v . At that time S_4 turns off, opening R_9 causing C_2 to discharge through G_2 increasing diode current. After C_2 is completely discharged, the voltage continues to decrease and the current and voltage decreases back to 0.

Model 3 shown in Figure II-6 like the previous models has elements V_1 , V_2 , V_3 , V_4 , L_s , R_s , C_1 , G_1 , G_2 , and BETA which need to be specified for each particular device.

TABLE II-3

MODEL 2 PARAMETER VALUES

<u>Parameter</u>	<u>TD-19</u>	<u>TD-13</u>	
V_1	0.0618	0.0618	volts
V_2	0.0682	0.0682	volts
V_3	0.249	0.249	volts
V_4	0.408	0.408	volts
G_1	0.161	0.0161	mho
G_2	0.0887	0.000887	mho
GM_1	0.0492	0.00492	
I_1	0.01	0.001	amp
I_2	0.00905	0.000905	amp

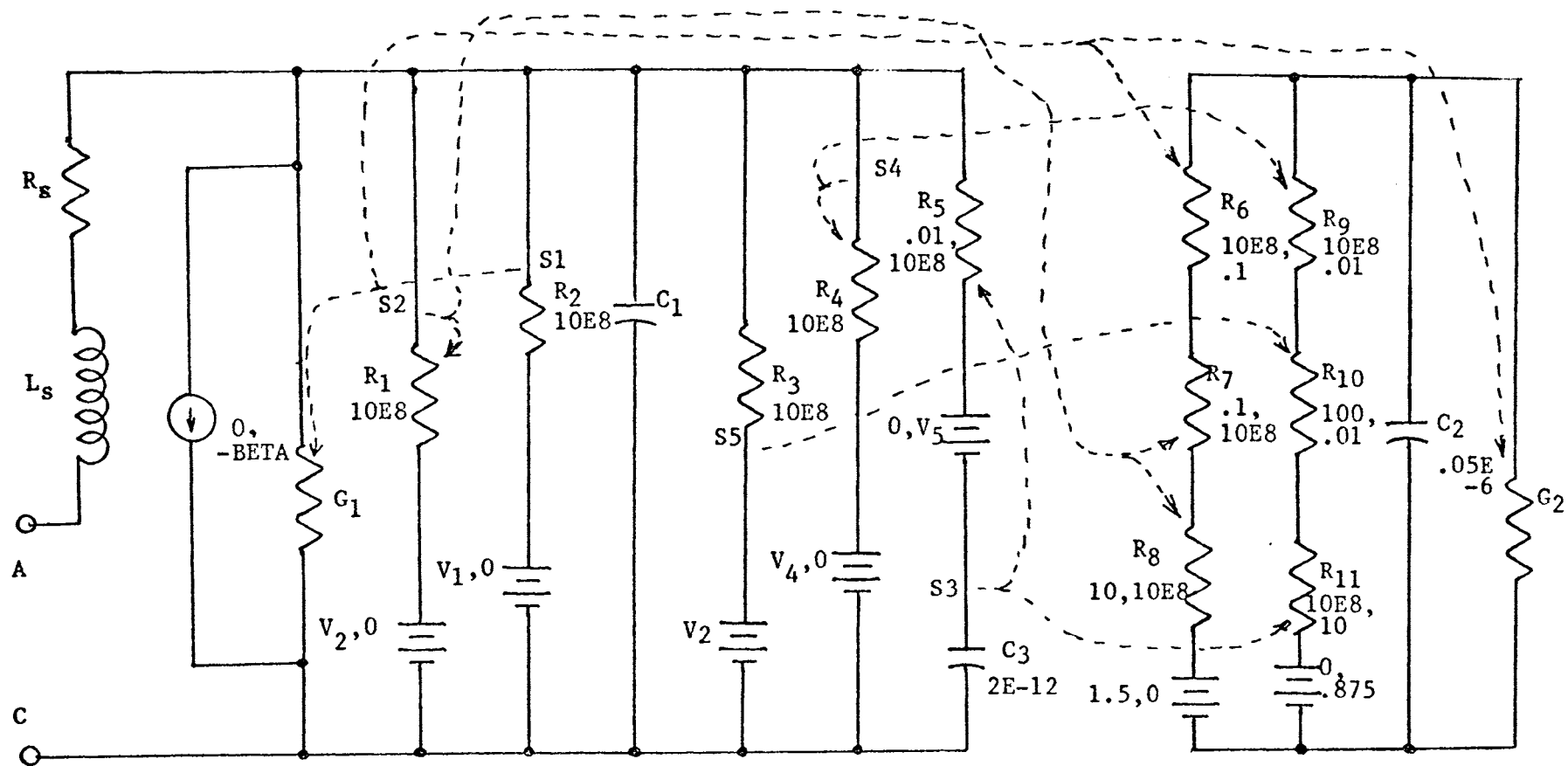


Figure II-6 Model 3

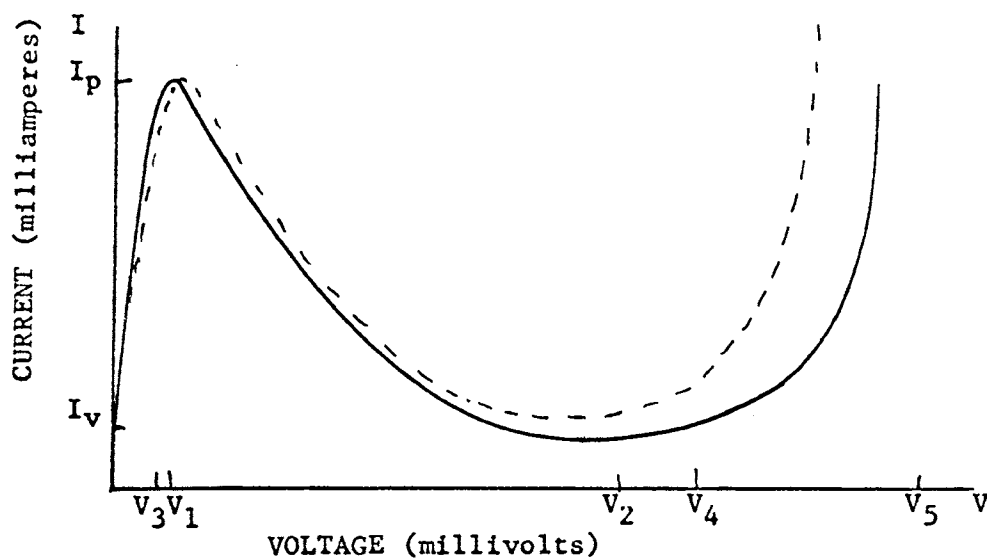


Figure II-7 Model 3 Current-Voltage Characteristic

The voltages V_1 , V_2 , V_3 , V_4 , V_5 and G_1 are as follows:

$$V_1 = V_p$$

$$V_2 = V_v$$

$$V_3 = .95V_p$$

$$V_4 = 1.15V_v$$

$$V_5 = V_{fp}$$

$$G_1 = \frac{I_p}{V_p}$$

G_2 and BETA are interrelated in this model by the following equation:

$$\frac{I_v}{V_1} = \left[\frac{1 - \exp\left(\frac{-t_v}{R_1 C}\right)}{R_1} \right] = \text{BETA} \left[\frac{1 - \exp\left(\frac{-(t_v - t_p)}{R_2 C}\right)}{R_2} \right]$$

where:

I_v = valley current

V_1 = Charging Voltage = 1.5 volts

$$R_1 = R_s + \frac{1}{G_2}$$

$$C = 0.05E-6$$

$$t_p = R C \ln \left[\frac{R_1 I_p}{V_1} - 1 \right] = \text{Time to Reach Peak Point}$$

The unknown quantities are:

BETA

$$R_2 = \frac{1}{G_2}$$

t_v = Time to Reach Valley Point

t_v is approximately a constant for a range of BETA's and G_2 's, therefore, to obtain an acceptable t_v set BETA=1 and $G_2 = 2G_1$ and run ECAP for the current-voltage. t_v is the time that S2 turned on. Then by picking values of BETA and solving for G_2 all the parameters for the model will be selected for Model 3 representing TD-19 are shown in TABLE II-4.

TABLE II-4

MODEL 3 PARAMETER VALUES

<u>Parameter</u>	<u>TD-19</u>	
V_1	0.065	volts
V_2	0.355	volts
V_3	0.0618	volts
V_4	0.408	volts
V_5	0.510	volts
G_1	0.154	mhos
G_2	0.308	mhos
BETA	-0.8	

BIBLIOGRAPHY

- ARRONS, M.W. and GOLDBERG, M.J. (1965) Computer Methods for Integrated Circuit Design, *Electro Technology*, May, vol. 75 no. 2, p. 77-81.
- CALAHAN, D.H. (1968) Computer-Aided Network Design, New York, McGraw-Hill, Inc., p. 245-273.
- CHRISTIANSEN, D. (1966) Computer-Aided Design Part 1: The Man-Machine Merger, *Electronics*, vol. 39 no.19, September 19, p. 110-123
- DANIEL, M.E. (1967) Development of Mathematical Models of Semiconductor Devices for Computer-Aided Circuit Design, *Proceeding of IEEE*, vol. 55 no. 11, November, p. 1913-1920.
- DAWSON, D.F. (1968) Computer-Aided Circuit Analysis by the Topological Approach, *Electro-Technology*, vol. 82 no. 5, November, p. 43-44.
- Digital Computer Program for Transient Analysis of Electronics Circuit (CIRCUS) (346-1), User's Guide, Seattle, Washington, Boeing Company, 1967, p. 90.
- EBERS, J. J. and MOLL, J. L. (1954) Large-Signal Behavior of Junction Transistors, *Proceedings of the IRE*, vol. 42 no. 12, December, p. 1761-1772.
- FALK, H. (1964) Computer Programs for Circuit Design, *Electro-Technology*, vol. 73 no. 3, March, p. 101-103, 162, 164.
- FALK, H. (1966) Computer Programs for Circuit Design, *Electro-Technology*, vol. 77 no. 6, June. p. 54-57.
- G.E. Transistor Manual, Seventh Edition, General Electric Company, 1964.
- GENTILE, S.P. (1962) Basic Theory and Application of Tunnel Diodes, D. Van Nostrand Company, Princeton, New Jersey, p. 295.
- GOLDBERG, N.J. and ARHARD, J.W. (1967) Computer-Aided Design: Part 7 Pergorming Non-Linear DC Analysis, *Electronics*, vol. 40 no. 5, March 6, p. 140-147.
- GUMMEL, H.K. (1968) A Charge-Control Transistor Model for Network Analysis Programs, *Proceeding of IEEE*, vol. 56 no. 4, April, p. 75.

- HALL, R.N. (1960) Tunnel Diodes, IRE Transactions on Electron Devices, vol. ed. 7 no. 1, January, p. 1-9.
- HAMILTON, D.J., LINDHOLM, F.A. and NARUD, J.A., (1964) Comparison of Large Signal Models for Junction Transistors, Proceedings of IEEE, vol. 52 no. 3, March, p. 239-248.
- HARBOURT, C.O. (1967) Computer-Aided Design: Part 5 Doing a Model Job, Electronics, vol. 40 no. 2, January 23, p.82-87.
- HINES, M.E. (1967) High Frequency Negative-Resistance Circuit Principles for Eaaki Diode Applications, The Bell System Technical Journal, vol. XLVI no. 3, March, p. 523-576.
- JENSEN, R.W. (1966) Charge Control Transistor Model for IBM ECAP, IEEE Transactions on Circuit Theory, vol. CT-13 no. 4, December, p. 428-437.
- JENSEN, R.W. (1967) A Network-Analysis Approach Simplifies the Problem, Electro-Technology, vol. 80 no. 5, November, p. 42-48.
- JENSEN, R.W., and LIEBERMAN, M.D. (1968) IBM Electronic Circuit Analysis Program Techniques and Applications, Englewood Cliffs, New Jersey, Prentice-Hall, Inc., p. 106-154.
- KUO, F.F. (1966) Network Analysis by Digital Computer, Proceedings of the IEEE, vol. 54 no. 6, June, p. 820-829.
- LINVILL, John G. (1958) Lumped Models of Transistors and Diodes, Proceedings of the IRE, vol. 46 no. 6, June, p. 1141-1152.
- LINVILL, John G. (1963) Models of Transistors and Diodes, New York, McGraw-Hill, Inc., p. 190.
- MAGNUSON, J.R. (1967) Computer-Aided Design: Part 8 Picking Transient Analysis Programs, Electronics, vol. 40 no. 8, April 17, p. 84-87.
- MALMBERG, A.F., CORNWELL, F.L. and HOFER, F.W. (1964) NET-1 Network Analysis Program. (709/94) Los Alamos Scientific Laboratory Report, September.
- MOLL, J.L. (1954) Large Signal Response of Junction Transistors, Proceedings of the IRE, vol. 42 no. 12, December, p. 1773-1763.

- RIPS, E.M. (1967) Calculating Amplifier Poles and Zeros with Digital Computer, *EEE*, vol. 15 no. 2, February, p. 94-100.
- ROBERTS, B.D. and HARBOUR, C.O. (1967) Computer Models of the Field-Effect Transistor, *Proceedings of IEEE*, vol. 55 no. 11, November, p. 1921-1929.
- Revised SCEPTRE user's Manual: Vol. 1, (AFWL-TR-67-124), Kirtland Air Force Base, New Mexico, International Business Machine Corp., April 1968.
- SCHEERER, W.G. (1968) Selecting Device Models for Computer-Aided Design, *Electro-Technology*, vol. 81, no. 55, May, p. 43-48.
- SOKAL, N.O., SIERAKOWSKI, J.J. and SIROTA, J.J. (1967) Part 1: Use a Good Switching Transistor Model, *Electronic Design*, vol. 15 no. 12, June 7, p. 54-59.
- SOKAL, N.O., SIERAKOWSKI, J.J., and SIROTA, J.J. (1967) Part 3: Diode Model is analyzed by Computer, *Electronic Design*, vol. 15 no. 14, July, p.80-85.
- SOMMERS, H.S. Jr. (1959) Tunnel Diodes as High Frequency Devices, *Proceeding of the IRE*, vol. 47 no. 7, July, p. 1201-1206.
- SPENCER, William (1969) Try this linear FET Model with ECAP, *Electronic Design*, vol. 17 no. 8, April, P. 82-85.
- SYLVAN, T.P. (1965) The Unijunction Transistor Characteristics, Application Note 90.10, General Electric, May, p. 95.
- WALL, H. (1966) Circuit Analysis by Computer, *Electro-Technology*, vol. 78 no. 5, November, p. 50-56.

VITA

The author, Carmon Dale Thiems, was born January 14, 1938, in Highland, Illinois. He received his primary and secondary education in Highland, Illinois. He received his college education from the University of Illinois in Urbana, Illinois. He received a Bachelor of Science Degree in Electrical Engineering from the University of Illinois in June, 1964.

He has been enrolled in the Graduate School of the University of Missouri - St. Louis since September of 1965.

171236